MAST-667 - Offshore Wind Power - Final Project

Wind and ocean power resources off the Florida coast, USA

University of Delaware – Spring 2005

Students: Felipe M. Pimenta, Berit Rabe, Ângela Spengler and Tiago Miranda
Prof. (Research leaders): Willett Kempton, Richard Garvine, Jeremy Firestone

(Final edition by: Felipe and Berit)

1) Introduction

In the last few years several scientific studies have emphasized the risks from anthropogenic greenhouse gases on the earth's climate and ecosystems. Recent studies show extreme changes where different scenarios are achieved using either models or experiments. For example, with an average temperature increase of Greenland by more than 3°C the global average sea level would rise 7 meters within the next 1000 years (Gregory *et. al* 2004). Larger pH changes than in the past 300 million years can occur over the next several centuries due to the ocean's absorption of CO_2, making the ocean more acidic. Effects will be seen on coral reefs, calcareous plankton and other organisms (Caldeira & Wickett 2003). Change in ocean carbon fixation rates and export pathways may also lead to a shift in algal community composition, as shown in experiments in the Bering Sea by Hutchins et al. (Hutchins 2005 *personal communication*). These examples are just a few possible outcomes of recent works. Different numerical model simulations on global climate change can be found in the Intergovernmental Panel on Climate Change (Church et al. 2001) and other works.

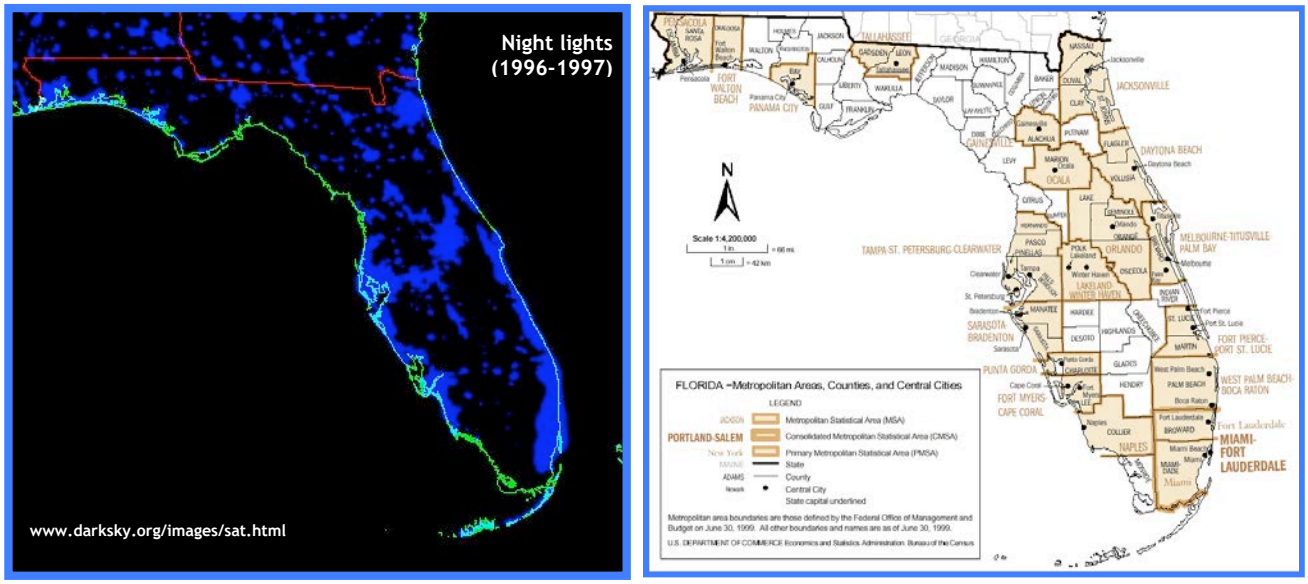

Figure 1) Left panel: Night lights in Florida from a satellite view indicating the main populated areas of the state of Florida. **Right panel**: Metropolitan areas, counties and central cities.

Due to these scenarios there has been simultaneously a great interest on renewable energy solutions that could help to reduce this threat consistently and supply the demands of growing markets.

Wind power appears as a promising and reliable source of renewable energy with wind as the world's fastest growing energy source. In the United States and Europe land-based wind parks have proven their efficiency. Wind currently provides more than 31,000 MW of electricity in about 40 countries. Despite of this, recent studies in the U.S. have shown that the resources in the U.S. may be substantially greater than previously estimated (Archer & Jacobson 2003). This further implies that the winds over possibly one quarter of the U.S. are strong enough to provide electric power at direct cost equal to that of a new natural gas or coal power plant.

Interestingly the wind resources over the seas are much higher, due to the absence of mountains, trees, buildings and other physical barriers. One good indicator is the growing market of design of wind turbines from big energy companies and the success of several offshore wind farms established in Europe. In the U.S. some organizations have been working on proposals, striving to build wind farms off the U.S. east coast. The

first offshore wind park in the U.S. is about to be built in Horseshoe Shoals, five miles off the Cape Cod shore in Massachusetts by Energy Management Inc[*]. It will consist of 130 wind turbines with a total maximum output of 420 MW. This project will lead the way for future projects, such as the Long Island Wind Project put forward by Bluewater Wind[†].

With more than 20,000 km of coastline, the U.S. offshore wind resources are still not very well known. A few places, like the northeast coast, have been mapped in more detail by Bailey & Brennan (2004) and private companies.

In this study we will focus on the possible resources of Florida. Florida is the 22nd largest state in the U.S., with a total area of 58,560 square miles. However, when comparing the size of the populations, Florida has the 4th national position, with a population of 15,982,378 residents, determined by the U.S. census of 2000. This census also established the population growth rate for Florida, from 1990 to 2000, as 23.53%. As can be seen in Figure 1, the coastal region of Florida is densely populated, favoring offshore wind power production with load centers close to the sites.

As for its electricity, Florida relies mostly on non-renewable sources of energy. In 2002, Florida generated 97% of its electricity from fossil fuels and nuclear power, and only 1% from renewable sources (Nayak 2005). Even considering all the environmental and public health impacts caused by the fossil fuels and nuclear power, and the fact that Florida could generate nearly one third of its total electricity usage from renewable energy, the policy still pushes towards the use of non-renewable sources of energy. More than $500 billion in federal subsidies have been placed in the oil and gas, coal and nuclear industries, and more than $35 billion were proposed by Congress in 2004 to be used as new subsidies for these industries. These new subsidies will represent a cost of more than $1.6 billion for Florida's taxpayers over the next ten years. Another issue in Florida is that the state does not have a renewable portfolio standard (RPS), which means that the state does not have a minimum amount of energy that has to be provided by renewable sources.

In this study attention will also be paid to the power production from ocean currents, since Florida has valuable resources from the Gulf Stream. This could be an alternative if the wind resource is not big enough or could be seen as a supplement to wind energy.

This report summarize the work conducted in the investigation of the Florida state offshore energy resource as part of the course, "Offshore wind power: Science, engineering and policy", conducted in the Spring of 2005 at the University of Delaware. The report is divided into the five following sections. In section two we will describe the methods used for wind data analysis and the results obtained by means of distribution maps and probability functions. Aspects about hurricanes and extreme meteorological events will be discussed in section three. The fourth section focuses on an alternative to offshore wind power: ocean currents. Marine protected areas are described in section five, and section six concludes with summary and conclusions of this report, with possible sittings favorable to the placement of new wind farms and ocean current parks.

[*] http://www.capewind.org
[†] http://www.bluewaterwind.com

2) Offshore wind power resource

2.1) Methods

2.1.1) Wind and bathymetric data

The wind data used in this work was obtained from the *National Data Buoy Center* (NDBC[‡]) website. The NDBC is a program operated by the National Ocean and Atmosphere Administration (NOAA) that is responsible for the development, design and maintenance of a network of data collecting buoys and coastal stations. Besides the real time data available on the Internet, the program offers a comprehensive historical data set. These data sets may contain meteorological data (e.g. wind speed, wind direction, pressure, temperature) as well as oceanographic measurements (e.g. temperature and salinity profiles, current measurements), depending on the considered stations. In the current study we selected wind information from 51 locations along the Florida coast. 25% of the wind measurements were obtained by meteorological weather stations in coastal sites and the other 75% were obtained by oceanographic buoys (Figure 2). The period of data coverage spans from 1973 to 2004, with most of the data collected in the late 1980's. From Figure 3 we can access the data availability over the years for each one of the considered stations. Most of the stations present more than two years of data coverage and some achieved more than 15 years in total. Although frequent gaps are found in these series its occurrence did not interfere with our analysis, which consists mostly of statistical estimations.

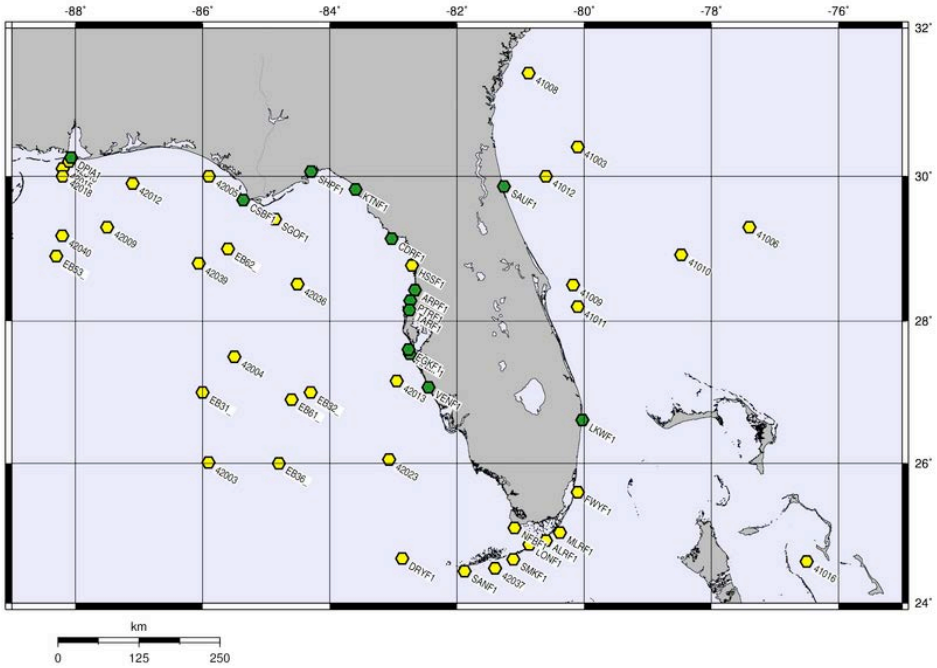

Figure 2) National Data Buoy Center wind stations for the Florida coast in the southeastern U.S. Yellow hexagons denote oceanographic buoys, whereas the green hexagons denote coastal stations. Station names are given by labels.

[‡]http://www.ndbc.noaa.gov

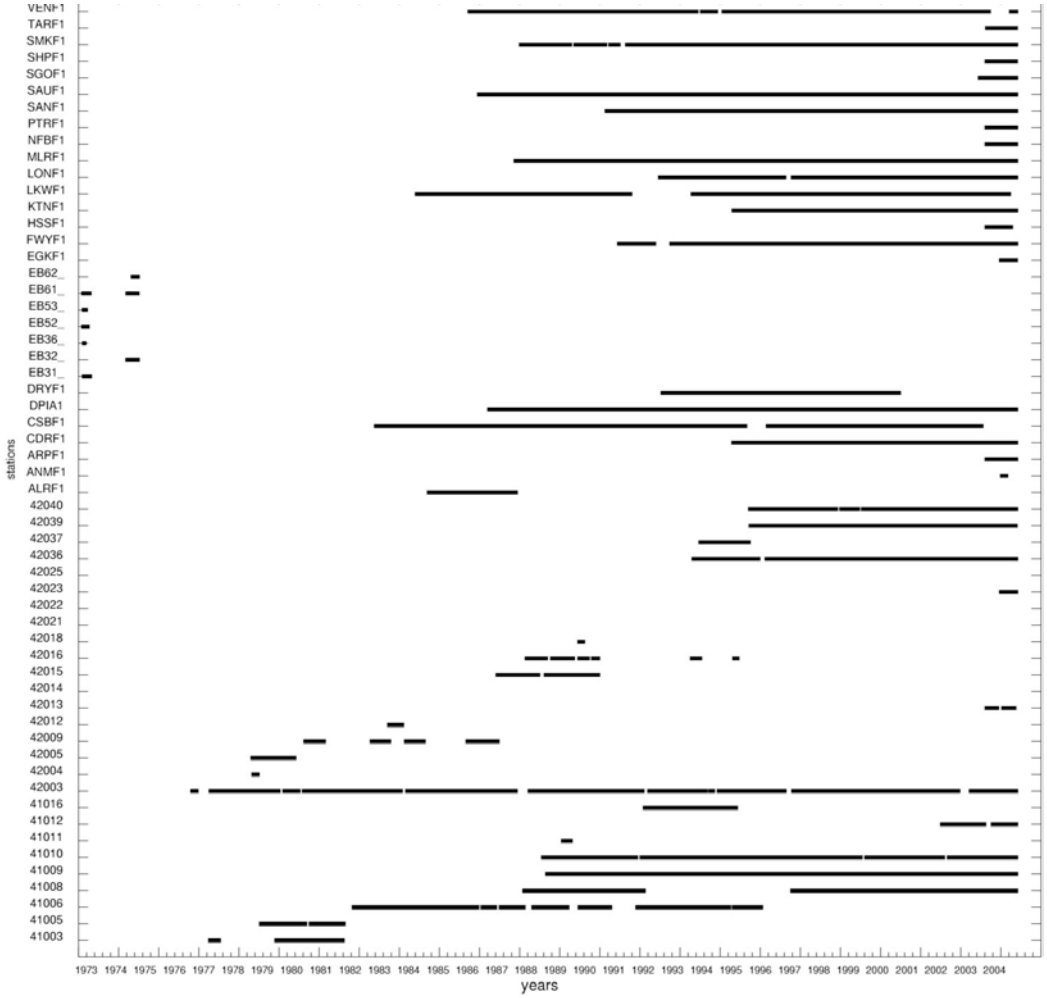

Figure 3) Meteorological data coverage for NDBC buoys for the Florida coast. Each square represents one data. (Stations 42014, 42012, 42022, 42025 were discarded due to absence of wind information. EB52 was discarded due to a mismatch in geographical position[§]).

The selected stations are mainly located between the coast and over the continental shelf as demonstrated by the bathymetric map in Figure 4. A considered number of them (~25%) are localized in deep waters (beyond 200 m).

As bathymetric information, we used data derived from the ETOPO-2 database, provided by the National Geophysical Data Center, on a resolution of 2 min. The bathymetric map shows how the west Florida presents a larger continental shelf, extending up to 200 km from the coast. For the specific needs of this work, we will be presenting the 20-meter isobath in the maps (denoted in Figure 4 by the red line). This depth represents the maximum depth today, in which the present technology is able to install offshore wind turbines. Overall, the area outlined between the coast and the 20-m isobath (henceforth denoted *inner-shelf)* is larger on the west, notably north of the Key West archipelago. The inner-shelf width varies from a few kilometers near the Miami coast up to 100 km on the northeastern and western part.

[§] Obs: We have contacted NDBC about the EB52 problem but without success in reply.

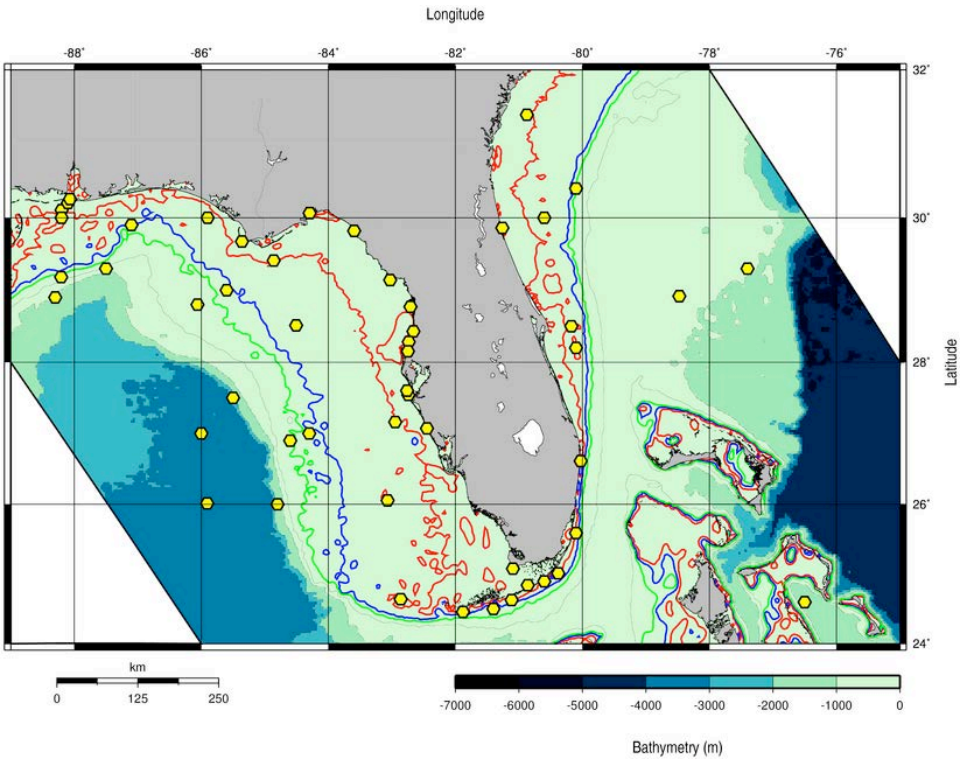

Figure 4) Florida shelf bathymetry and wind stations. The 20-m isobath is indicated by the red line and the 100 and 200-m isobaths by the blue and green lines respectively. Note the larger difference of shelf widths between the west and east coasts and the higher concentration of wind stations in coastal and shelf areas. (Source: ETOPO-2 data set from the National Geophysical Data Center).

Our main interest will especially focus on the inner shelf, where wind resources might be explored in the near future. Due to the relatively good number of coastal and deep-water stations, we decided to work with all wind speed data available as an aid for interpreting the spatial distributions of the data. We also worked with all wind data series, independent of their length. Their data coverage though will be clearly identified in the maps and results of the analysis.

A list of all the station codes as well as their geographical positions, total data coverage length and their anemometer heights can be accessed in Table 1.

2.1.2) Logarithmic wind speed profile (log law)

In wind energy studies generally there is the need to estimate the wind velocity at different heights from a reference level of measurement, here denoted as z_{ref}. For this study, before performing any analysis we must estimate the wind speed at the wind turbine hub height of 80 m. This procedure is especially important because the winds are measured at different heights according to the considered station (Figure 5).

Our approach will follow the log law, which has its origins in studies of boundary layer flow in fluid mechanics and in atmospheric research. Its final form is a result of a combination of empirical and theoretical research. The derivation of the formula is beyond the scope of this work, but a good description can be found in Manwell *et al*. 2002. The log law states that the velocity at 80 m (V_{80m}) can be computed simply by the following equation, where V_{ref} is the wind velocity measured at our wind station at the height z_{ref}:

$$V_{80} = V_{ref} \frac{\ln(80) - \ln(z_o)}{\ln(z_{ref}) - \ln(z_o)} \quad \text{(Eq.1)}$$

The parameter z_o is called the *surface roughness* and its length depends strongly on the terrain type. For calculations over open sea (see our yellow hexagons in Figure 5 or Table 1) we used z_o=0.35 mm, whereas for the terrestrial stations (green hexagons on Figure 5) we assumed z_o=100 mm. These values were obtained from the literature (Manwell *et al*. 2002). Once the wind values are referenced to 80 m we are able to perform further computations and comparisons that will be described along the report.

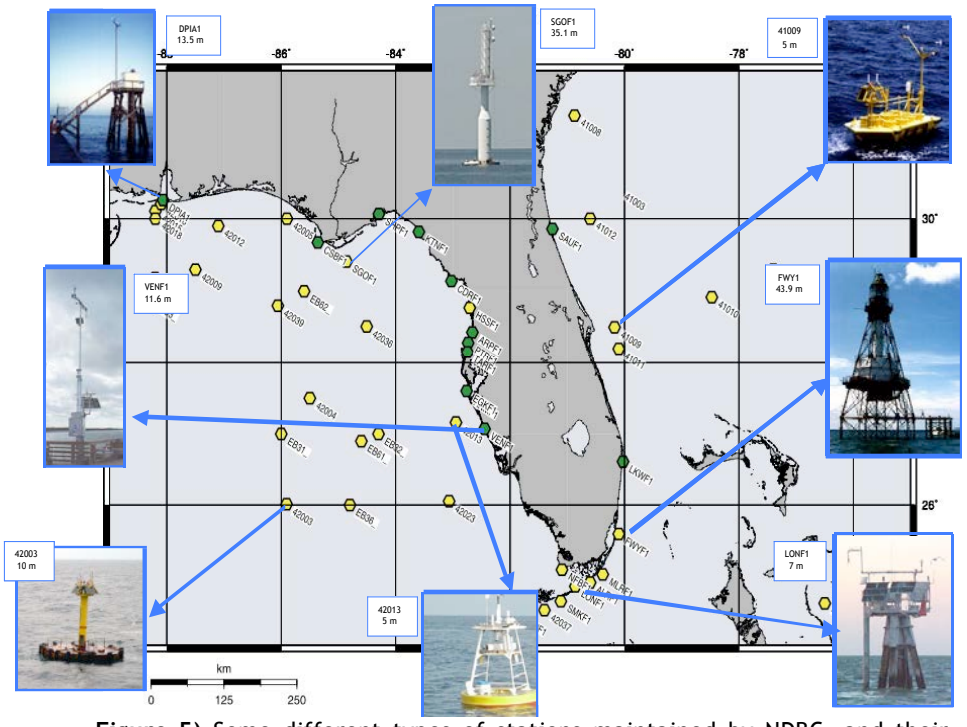

Figure 5) Some different types of stations maintained by NDBC, and their respective anemometer heights.

2.1.3) Available wind power

Besides analyzing the wind velocity distribution it is useful to observe this resource in terms of wind power density (W/m^2). Its short derivation, described in Manwell et al. (2002), comes from the assumption of the mass flow of air through a rotor disk of area "A" given in terms of the wind velocity at 80 meters height: $dm/dt = \rho A V_{80}$, where ρ is the air density (1.225 Kg.m^{-3}). From the flux of mass, the kinetic energy associated with the wind (namely, the power of the flow) can be derived as: $P = \frac{1}{2}\frac{dm}{dt}(V_{80})^2$. In conclusion, the wind power density consists of its distribution per unit area (P/A), which results in an expression proportional to the cube of the wind velocity:

$$P_{80} = \frac{1}{2}\rho(V_{80})^3 \quad \text{(Eq.2)}$$

Note that the actual power production for a wind turbine must also take into account the fluid mechanics of

the flow passing through a power producing rotor, the aerodynamics and efficiency of the rotor/generator combinations. In practice it is suggested that a maximum of 45% of the available wind energy can be harvested by the best modern wind turbines (Manwell et al., 2002). Finally we will be computing the average and standard deviations of wind power density for each of the stations by equations 3a and 3b, where N denotes the number of observations considered in the average:

$$\overline{P}_{80} = \frac{\rho}{2}\frac{1}{N}\sum_{i=1}^{N} V_{80}(t_i)^3 \quad \text{and} \quad \sigma_{P_{80}} = \sqrt{\frac{1}{N-1}\sum_{i=1}^{N}\left[P_{80}(t_i) - \overline{P}_{80}\right]^2} \quad \text{(Eq.3a,b)}$$

2.1.4) Rayleigh distribution

The likelihood that the wind speed has a particular value can be described in terms of a probability density function (pdf). One way to define the probability density function $p(V_{80})$ is that the probability of a wind speed occurring between U_a and U_b is given by:

$$P(V_a < V_{80} < V_b) = \int_{Va}^{Vb} p(V_{80})dV \quad \text{(Eq.4)}$$

The total area under a probability distribution curve is necessarily one. The Rayleigh distribution is one of the simplest wind velocity probability distributions to represent the wind resource, since it requires only knowledge of the mean wind speed. Its probability density function is given by the following equation with V denoting the wind speed:

Rayleigh distribution

$$p(V) = \frac{\pi}{2}\left(\frac{V}{\overline{V}^2}\right)\exp\left[-\frac{\pi}{4}\left(\frac{V}{\overline{V}}\right)^2\right]$$

(Eq.5)

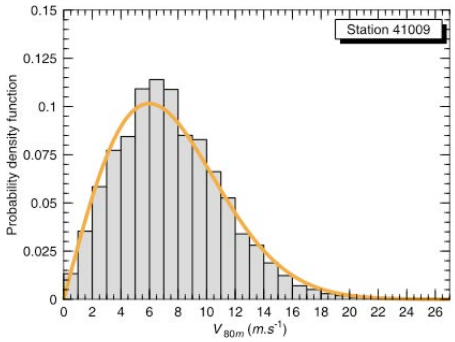

Figure 6: A typical wind speed histogram and its Rayleigh probability distribution. The bin width of the histogram is 1 m.s^{-1}. The histogram was created based on a series of 24 years of data for station 41009.

Perhaps a good way to grasp the idea behind the pdf distribution is by observing it jointly with a typical wind speed histogram distribution, as in Figure 6. In this figure, the gray bars indicate the percentage of occurrence divided into wind speed classes, centered at specific velocities (here the width of each bar is given by 1 m.s^{-1}). The area of each bar represents then the percentage of our data distribution found between its lower and upper limits. As an example, for a bar centered at V_{80}=3.5 m.s^{-1} we conclude there is 7.5% probability of observing winds between 3 and 4 m.s^{-1}. The continuous orange line represents the Rayleigh distribution for the same data set.

We can therefore access the probability of occurrence of wind speeds between prescribed limits by applying the integral of Equation 4, which measures the area beneath the Rayleigh curve. In this work, we will use the Rayleigh distribution jointly with the wind power production curves known for the GE offshore wind turbine, presented in a subsequent subsection. From the Rayleigh distribution we are able to compute cumulative distributions by integrating the function from ∞ to 0 - or heuristically by cumulatively summing up the histogram bars from the right to the left. The resultant function gives us the probability of occurrence of winds at least at a certain velocity.

2.1.5) Wind turbine characteristics

In order to map and provide estimations based on the specific characteristics of the available technology of wind turbines, we will make use of the operating data and power curve from the *General Electric 3.6s Offshore wind turbine (GE3.6s)* (Figure 7). The *GE3.6s* was specially designed for oceanic operations with a minimal necessity of periodical maintenance and has been used in offshore wind farms in Europe.

The turbine has three blades, with a diameter of 104 m and a swept area of 8495 m^2. Its hub height might vary from one location to another (e.g. depending on the wave heights and water depth) but its average height is 80 m. The turbine cut-in and cut-out wind speeds are 3.5 and 27 $m.s^{-1}$ respectively, which means that the turbine starts to generate power at 3.5 $m.s^{-1}$ and stops generating when the wind speed surpass 27 $m.s^{-1}$. The maximum power generation (3.6 megawatts (MW)) occurs for wind speeds above 14 $m.s^{-1}$.

GE 3.6s offshore	
Operating data	
Rated capacity	3.600 kW
Cut-in wind speed	3.5 $m.s^{-1}$
Cut-out wind speed	27 $m.s^{-1}$
Rated wind speed	14 $m.s^{-1}$
Rotor	
Number of blades	3
Rotor diameter	104 m
Swept area	8.495 m^2

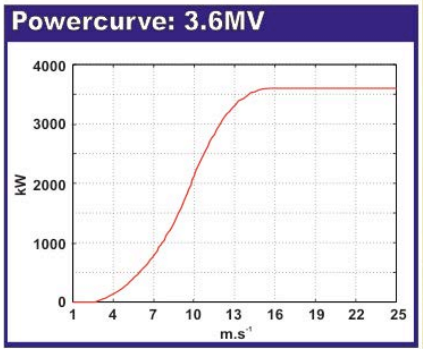

Figure 7) GE wind turbine *GE3.6s offshore* characteristics and power curve as a function of wind speed. The photo shows a turbine installed on the east coast of Sweden (http://www.gepower.com/prod_serv/products/wind_turbines/en/36mw/index.htm)

The curve seen in Figure 7 will provide us with a direct measure of the turbine production as a function of wind speed at 80 m (V_{80}). Observe that this curve is a result of the turbine design as it tries to maximize the power gain for wind velocities ranging "on the slope" of the curve.

2.1.6) Turbine power production from wind data

Once we present the wind speed probability density function and the machine power production curve, our objective here will be to explain how we may obtain cumulative probability distribution curves for wind power generation. Figure 8 will help to summarize some of these ideas.

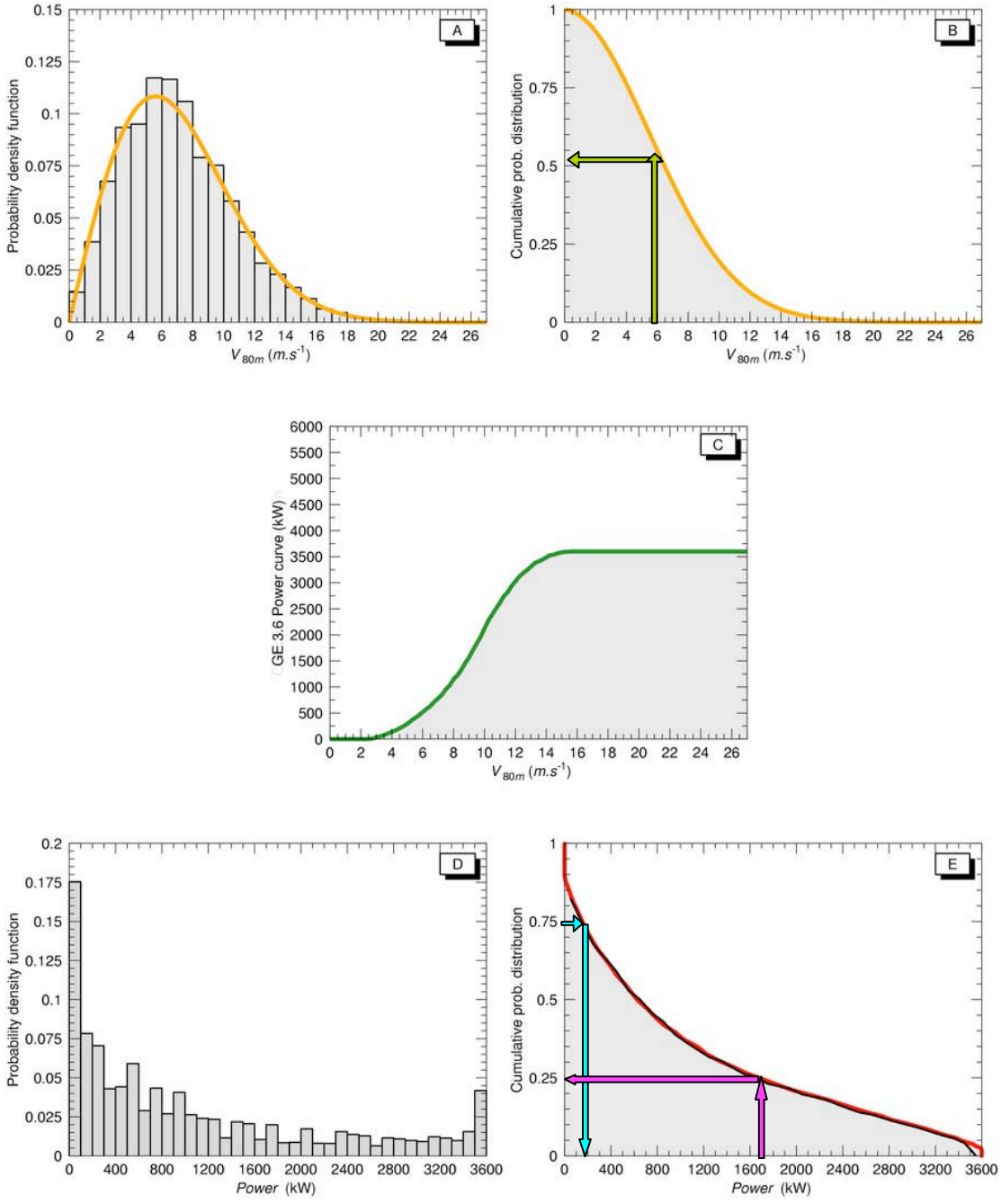

Figure 8) A: Wind speed histogram and Rayleigh probability density function. **B:** Cumulative probability distribution derived by the integration of "A" curve. **C:** *GE3.6s* wind turbine power curve. **D:** Power production histogram. **E:** Cumulative probability distribution of graph "D". The data used for computing these graphs corresponds to station 41008.

Recall from a previous section that the probability density function (pdf) can be integrated through its role domain yielding a cumulative probability distribution. In other words we can start from graph "A" of Figure 11 and perform a numerical integration $\int_{\infty}^{0} p(V_{80})dV$ (or heuristically, perform the sum of the histogram bars from right to left) and obtain the cumulative function displayed in graph "B". This last curve gives us the probability (or fraction of time) that observed winds are ***greater or equal*** than a specified velocity. As an example from this graph, we have a ~50% chance of occurrence of winds that have at least of 6 $m.s^{-1}$ (see green arrows on graph "B").

The same idea can be extended in terms of power production from a wind turbine once we know the relation of power production to wind speed. This relation gives the power production function which is plotted on graph "C".

In the same way we constructed a wind speed histogram, we can construct a "power generation" histogram by computing for each velocity measurement $V_{80}(t_i)$ at time t_i its respective power generation $P_{turb}(t_i)$ (MW). By classifying the P_{turb} series according to classes, we are able to build another histogram, as depicted in graph "D" of Figure 8. In this graph the area under each bar represents the probability of power generation by the turbine.

Now, in the same way we constructed a cumulative histogram from "A to B", here we propose a "cumulative histogram" from "D to E" given by the black line in graph "E". This last step allows us to draw some conclusions in terms of probability, but now in terms of "generated power". The arrows in this graph exemplify its use. From the "magenta arrows" we can conclude that this site will have a 25% chance of generating ***at least*** 1.8 MW. If it is desirable to increase the confidence and hence the probability to say 75%, we observe that there is a considerable reduction in terms of production. Our expectation is then to be able to generate ***at least*** 0.2 MW 75% of time (blue arrows).

In the section of results, rather than analyze these cumulative power production curves for each station, we will try to analyze them in terms of known average values determined for by the wind classes. That will be done by producing the cumulative histograms directly from the Rayleigh distributions, as is seen in this case by the red line on graph "E".

2.2) Results

2.2.1) Spatial analysis of wind resource

Looking now at spatial distributions; maps of average wind speed, time of activity of the stations and wind power density will be analyzed. The data acquired from buoys and land stations was used to generate maps of average wind speed at 80 m height in two different ways (Figure 9). A classification between different wind classes at 80 m after Archer and Jacobsen (2003) is made to observe the wind class at each specific station in combination with length of data coverage. The other way entails presenting the average wind speed at 80 m in an interpolated contour map with the average velocity at each station. Wind distribution here is given for the average of the data series.

In order to avoid misinterpretation, refer to the upper map whenever necessary. Its labels represent the extent in years of the data coverage used for calculating the mean wind speed.

Existing wind classes in the waters around Florida are classes one through four; higher wind speeds and therefore higher wind classes could not be identified. For offshore wind power production a higher wind class would be favorable.
Class four winds appear far offshore at two stations in the Atlantic, three offshore stations in the Gulf of Mexico, and one station close to Panama City. Data coverage, denoted by the labels, shows not even a one-year data coverage for this station. Though five stations to the west of this station show data coverage of up to 17.46 years. These stations are all categorized as wind class three, making a wind class four station in that

region reasonable.
Along the Atlantic coast winds are in general stronger with a few stations in the wind range from 6.9 to 7.5 $m.s^{-1}$ (class three), all of them showing good data coverage. One station off the coast of Jacksonville with a data collection period of 11.47 years, also shows a wind class three category and will be further mentioned later in the discussion in combination with policies regarding Jacksonville.

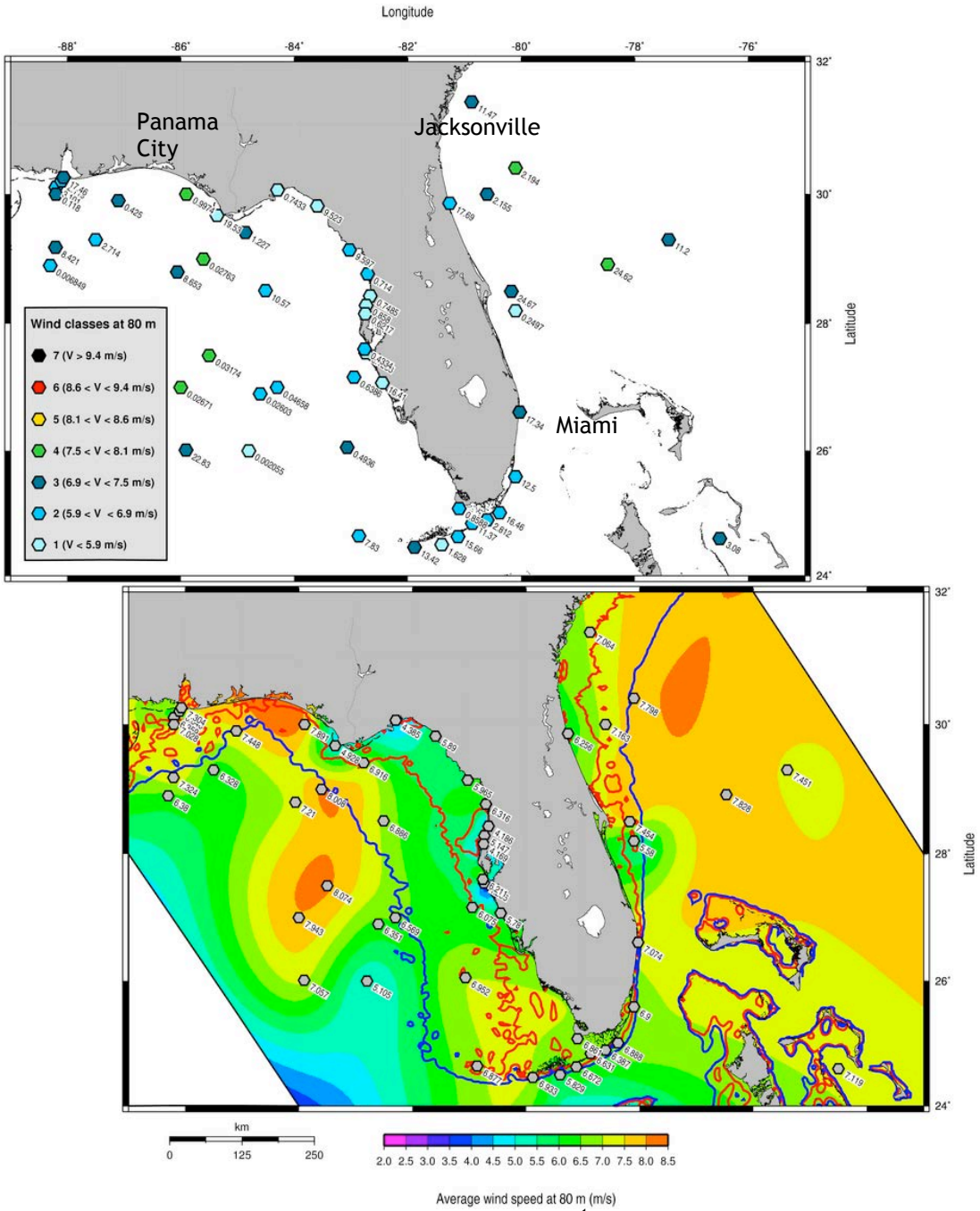

Figure 9) Average wind speed at 80 m (V_{80} $m.s^{-1}$). **Upper map:** Wind classes at 80 m are given in colors and the labels denote the data coverage in years. **Lower map:** Contoured map produced from the average wind speeds. Labels indicate the average V_{80} and colors indicate the wind intensity, ranging from 2 $m.s^{-1}$ (purple) to 8.5 $m.s^{-1}$ (orange). The tick blue/red line indicates the 20-m/100-m isobaths.

From analysis of the lower map from Figure 9 it is possible to identify more intense (>6.5 $m.s^{-1}$) wind areas as opposed to single stations as in the upper figure. These regions of higher winds occur along the east coast inner-shelf, in the southern area between the continent and the Key West Archipelago, and at the southern region of the coast between Panama City and Pensacola extending south to deep waters.

The extent of the inner-shelf should be observed. The southeast coast's very narrow inner-shelf could be an impediment for wind turbine installation while in the northeast the 20-m isobath occurs farther from the coast. The west coast has the advantage of a larger inner-shelf, including some of the more intense wind areas in shallower waters.

The wind turbines time of activity were estimated by the percentage of time the wind favors wind power generation, namely the relative amount of time we found winds between 3.5 and 27 $m.s^{-1}$. Figure 10 shows this percentage of time of activity for each station, with labels indicating the exact % values. The correlation with more intense wind areas is in a reasonable accordance with areas of large activity. Values range from 47% to 90%, with regional differences. Around Jacksonville in the northeast, percentages of around 80% occur. The Key West area has even higher percentages. Also the far west end of the Florida coast on the Gulf of Mexico shows values favorable for wind power production, being 78 – 87 % of the time between 3.5 and 27 $m.s^{-1}$. Lowest values occur along the west coast between 28° and 30° N.

The calculated average wind power density can give us specific information on the power content associated with the wind for each area. Figure 11 shows how wind power density is associated with the higher wind incidence sites. Standing out is one station (namely EB31, see Figure 2) in deep waters in southwest Florida. High wind power density there is believed to be due to the high average wind speed data collected in a small time series (0.02671 year, as can be seen in Table 1 and in Figure 9) giving some inconsistency to the information for this site. Besides this station the wind power density can be categorized into different region. Higher values occur along the northeast coast on the Atlantic coast and around the Panama City region. Poorest wind power density is found along the west coast between 28° and 30° N with only 100 to 200 $W.m^2$. The Key West area shows medium wind power densities in the order of 300 $W.m^2$. Therefore it can be seen that fluctuations from about 100 to 450 $W.m^2$ can occur in the Florida region.

All these results are summarized in Table 1 showing geographical position, percentage of time activity, average and standard deviation of wind speed at 80 m, data coverage in years, average wind power density with standard deviation, anemometer height and classification between land and sea station, as well as the average GE power production with standard deviation.
Having focused on station 41008 right off the coast of Jacksonville (see circle in Figure 10), we can get the following information from the table for this station (see red rectangle in Table): the position is at 80.87°W and 31.4°N, it is active 83.61 percent of the time with an average wind speed at hub height of 7.064 $m.s^{-1}$ (standard deviation of 3.597 $m.s^{-1}$) and data coverage of 11.47 years. The wind power density is given by 403.4 $W.m^{-2}$ (standard deviation of 645.2 $W.m^{-2}$) and the anemometer height is 5 m, being a sea station. The average GE power production is given by 1083 kW (standard deviation of 1091 kW). This information can be accessed for individual station, and is a good source for a quick overview.

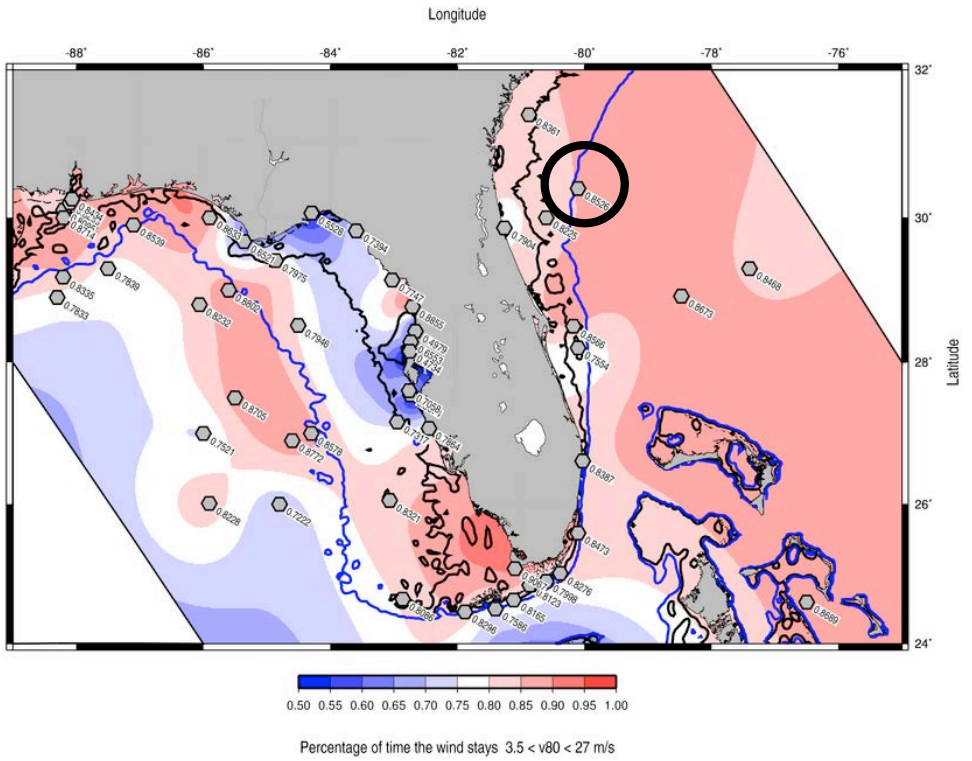

Figure 10) Time of activity of the wind turbine derived from the percentage of time the wind speed remains between $3.5 < V_{80}$ ($m.s^{-1}$) < 27. Labels indicate the exact % value at each station. The shades of colors indicate the percentual ranging from 50% (blue) to 100% (red). The tick black/blue line indicates the 20-m/100-m isobaths.

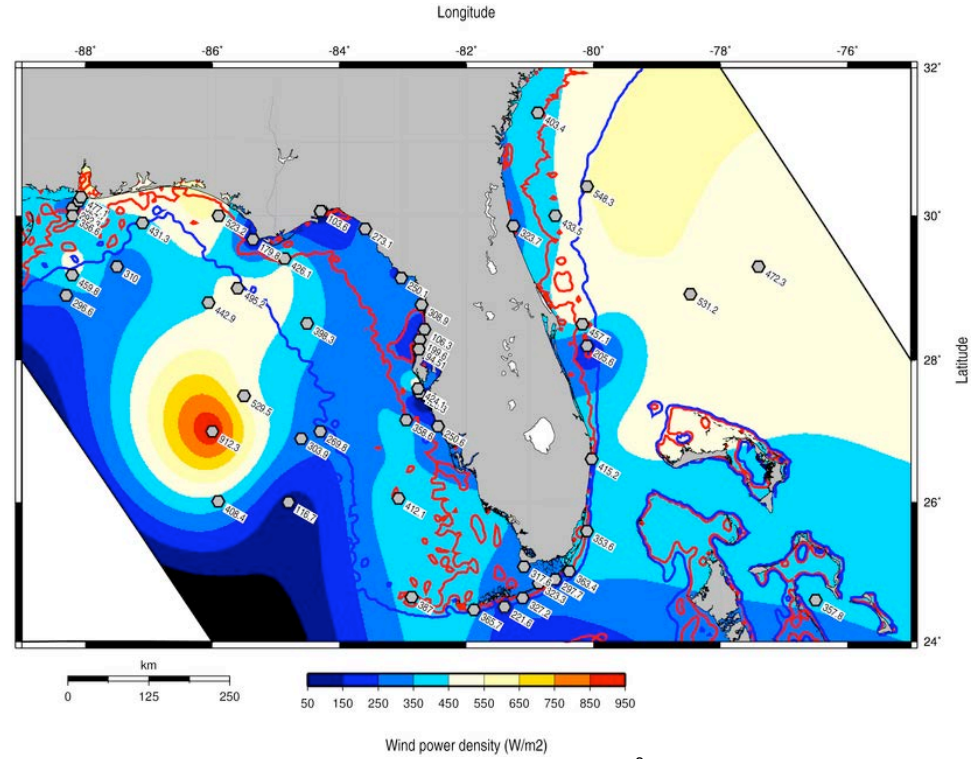

Figure 11) Wind power density at 80 m (average P_{80} $W.m^2$, see Eq. 3a). Labels indicate the exact values of P_{80} at each station. The color bar indicates the wind power ranging from 50 $W.m^2$ (dark blue) to 950 $W.m^2$ (red). The tick red/blue line indicates the 20-m/100-m isobaths.

2.2.2) Spatial and probability analysis of power production

Here we first present the results for the computation of a "virtual" power production for each site for which we have wind measurements. To accomplish this, we make use of the *GE3.6s* wind turbine power curve presented in Figure 7 in order to "translate" our wind values in terms of hourly values power production. Once we converted the wind values to a series of power production, the resultant averaged values for each station were plotted in Figure 12.

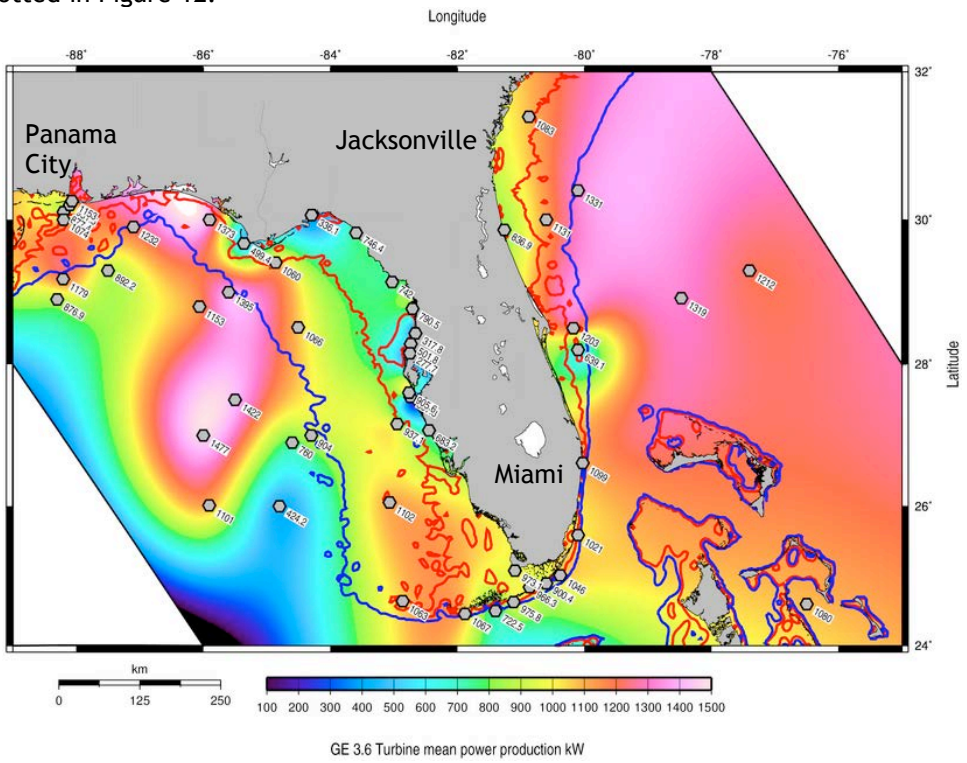

Figure 12) Average power that would be produced by the *GE3.6s* wind turbine, taking into account the power curve distribution and all available wind data series. The color bar indicates the wind power ranging from 100 kW (dark blue) to 1500 KW (white). The tick red/blue line indicates the 20-m/100-m isobaths. Labels indicate the actual value for each site in kW.

From the map we can identify the coasts off Pensacola and Miami as fairly good sites for power production (with values around 1 and 1.1 MW). The region near Jacksonville has a coastal wind station indicating not very promising resources near land (~0.8 MW), but its offshore stations indicate a better potential near the 20 m depth, with values of the order of 1 to 1.3 MW. The poorest region, with average production around 0.3 MW was found on the west coast between 27 and 30^{o} latitude. These values don't represent the inner-shelf resource well though, since most of them were measured by land stations and the nearest offshore station is 175 km off coast (see Figure 2). The higher value found for station EB31 should again be analyzed with some caution, since it represents a very small time series of data. The stations along Key West demonstrate an average production of nearly 0.7 up to 0.9 MW, being the best results found for the stations near the end of the archipelago (see station DRYF1 ~ 1.06 MW).

Although these distributions are quite useful for relative comparisons or indication of our "best site candidates", one should be aware of the large fluctuations that arise from the estimated production by these turbines. In Table 1 we can observe for each station the average and standard deviations of these power productions. Standard deviations have large values, comparable to the means.

A look on a short time series might illustrate these large deviations from the mean (Figure 13). In this figure we present the wind velocity time series together with the computed power production for the station 41008. As seen the power production has very large fluctuations in a matter of days.

Station name	Longitude (degrees)	Latitude (degrees)	% Time active	Average V_{80} m.s^{-1}	Stand dev. V_{80} m.s^{-1}	Data cover. (years)	Average P_{80}(W.m^{-2})	Stand. dev. P_{80}(W.m^{-2})	Anem. height	Sea(1) Land(0)	Ave. power P_{turb} (kW)	Std power P_{turb} (kW)
41003	-80.1	30.4	0.8526	7.798	4.083	2.194	548.3	781.9	5	1	1331	1223
41006	-77.4	29.3	0.8468	7.451	3.819	11.2	472.3	725.4	5	1	1212	1144
41008	-80.87	31.4	0.8361	7.064	3.597	11.47	403.4	645.2	5	1	1083	1091
41009	-80.17	28.5	0.8566	7.454	3.679	24.67	457.1	702.2	5	1	1203	1127
41010	-78.47	28.92	0.8673	7.828	3.884	24.62	531.2	803.5	5	1	1319	1175
41011	-80.1	28.2	0.7554	5.58	2.923	0.2497	205.6	352.3	5	1	639.1	799.1
41012	-80.6	30	0.8225	7.163	3.783	2.155	433.5	691	5	1	1131	1120
41016	-76.5	24.6	0.8689	7.119	3.151	3.08	357.8	468.6	10	1	1080	982.4
42003	-85.91	26.01	0.8228	7.057	3.668	22.83	408.4	752.8	10	1	1101	1096
42004	-85.5	27.5	0.8705	8.074	3.666	0.03174	529.5	606.5	10	1	1422	1231
42005	-85.9	30	0.8633	7.891	3.822	0.9974	523.2	668.7	10	1	1373	1200
42009	-87.5	29.3	0.7839	6.328	3.463	2.714	310	498.6	10	1	892.2	1008
42012	-87.1	29.9	0.8539	7.448	3.553	0.425	431.3	532.5	10	1	1232	1108
42013	-82.95	27.16	0.7317	6.075	4.217	0.6386	358.6	695.6	5	1	937.1	1087
42015	-88.2	30.1	0.8095	6.359	3.251	3.101	292.3	439.8	5	1	877.4	960
42016	-88.1	30.2	0.8299	6.646	3.283	2.119	324.7	481.9	5	1	951.5	1001
42018	-88.2	30	0.8714	7.028	3.236	0.118	356.6	445.5	5	1	1074	1054
42023	-83.07	26.05	0.8321	6.952	3.881	0.4936	412.1	610.4	5	1	1102	1124
42036	-84.51	28.51	0.7946	6.886	3.757	10.57	398.3	625.1	5	1	1066	1124
42037	-81.4	24.5	0.7586	5.829	2.951	1.628	221.6	313.3	5	1	722.5	833.4
42039	-86.06	28.8	0.8232	7.21	3.816	8.653	442.9	713.1	5	1	1153	1144
42040	-88.21	29.18	0.8335	7.324	3.825	8.421	459.8	805.3	5	1	1179	1144
ALRF1	-80.6	24.9	0.7998	6.387	3.304	2.812	297.7	450.5	47.5	1	900.4	963.3
ANMF1	-82.74	27.54	0.5674	4.286	2.79	0.1203	125.3	333.5	10.8	0	367.8	629.4
ARPF1	-82.66	28.43	0.4979	4.186	2.452	0.7485	106.3	315.7	10.3	0	317.8	576.7
CDRF1	-83.03	29.14	0.7747	5.965	3.067	9.597	250.1	489.2	10	0	742	881.6
CSBF1	-85.36	29.67	0.6521	4.928	3.016	19.53	179.8	501.7	9.8	0	499.4	763.2
DPIA1	-88.07	30.25	0.8434	7.304	3.921	17.46	477.1	961.5	13.5	0	1153	1158
DRYF1	-82.86	24.64	0.8086	6.877	3.683	7.83	387	623.8	5.7	1	1063	1096
EB31_	-86	27	0.7521	7.943	5.651	0.02671	912.3	3586	10	1	1477	1329
EB32_	-84.3	27	0.8578	6.569	2.793	0.04658	269.8	297.1	10	1	904	874.8
EB36_	-84.8	26	0.7222	5.105	1.975	0.002055	116.7	113.5	13.8	1	424.2	419.4
EB53_	-88.3	28.9	0.7833	6.38	3.315	0.006849	296.6	436.1	13.8	1	876.9	959.1
EB61_	-84.6	26.9	0.8772	6.351	2.997	0.02603	303.9	1274	13.8	1	760	723
EB62_	-85.6	29	0.8802	8.008	3.48	0.02763	495.2	550.2	13.8	1	1395	1139
EGKF1	-82.76	27.6	0.7058	6.211	4.383	0.4334	424.1	1249	10	0	905.6	1102
FWYF1	-80.1	25.59	0.8473	6.9	3.299	12.5	353.6	769.2	43.9	1	1021	1011
HSSF1	-82.71	28.77	0.8855	6.316	3.21	0.714	308.9	808.2	6.6	1	790.5	908.5
KTNF1	-83.59	29.82	0.7394	5.89	3.365	9.523	273.1	566.7	10	0	746.4	946.7
LONF1	-80.86	24.84	0.8123	6.631	3.327	11.37	323.3	485.7	7	1	966.3	986.4
LKWF1	-80.03	26.61	0.8387	7.074	3.7	17.34	415.2	691.4	13.7	0	1099	1111
MLRF1	-80.38	25.01	0.8276	6.888	3.453	16.46	363.4	597.1	15.8	1	1046	1045
NFBF1	-81.09	25.08	0.9067	6.861	2.952	0.8588	317.6	444	5.5	1	973.1	935.5
PTRF1	-82.73	28.28	0.6553	5.147	2.951	0.858	199.6	724.2	10.1	0	501.8	747.4
SANF1	-81.88	24.46	0.8296	6.933	3.45	13.42	365.7	527.7	13.1	1	1067	1050
SAUF1	-81.26	29.86	0.7904	6.256	3.524	17.69	323.7	701.5	16.5	0	836.9	1010
SGOF1	-84.86	29.41	0.7975	6.916	3.909	1.227	426.1	754.6	35.1	1	1060	1139
SHPF1	-84.29	30.06	0.5528	4.385	2.294	0.7433	103.6	219	10	0	336.1	555.5
SMKF1	-81.11	24.63	0.8165	6.672	3.311	15.66	327.2	534.6	48.5	1	975.8	994.4
TARF1	-82.75	28.15	0.4734	4.169	2.194	0.6217	94.51	305.7	7	0	277.7	483.9
VENF1	-82.45	27.07	0.7864	5.78	3.164	16.41	250.6	565.9	11.6	0	683.2	885.6

Table 1) Wind stations geographical positions, percentage of time of activity (given by the time the wind remains between 3.5 < V_{80} m.s^{-1}< 27), average and standard deviations of wind speed at 80 m (V_{80} m.s^{-1}), data coverage in years, average and standard deviation of the wind power density (P_{80} W.m^{-2}), anemometer height (m), and average and standard deviation of the estimated *GE3.6s* turbine power production (P_{turb} kW).

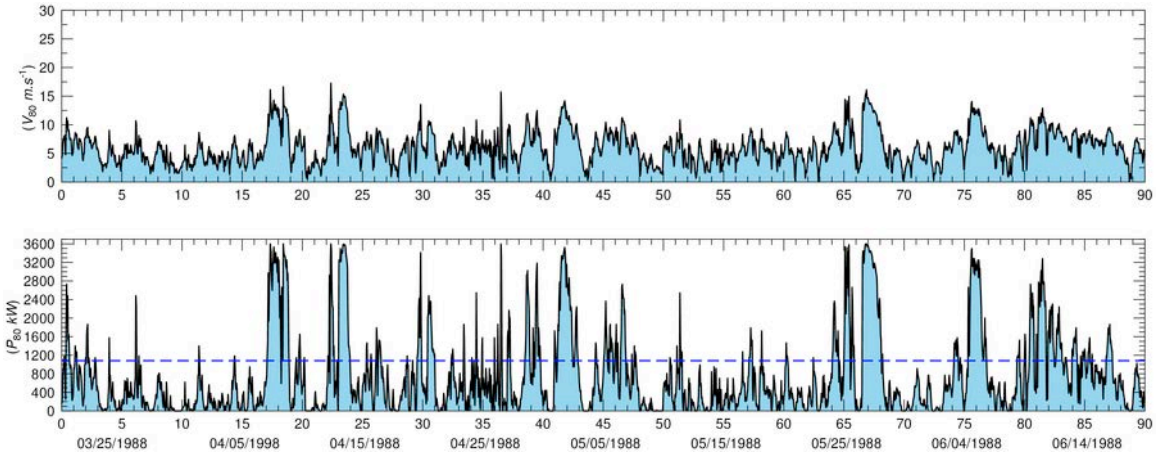

Figure 13) Top panel: Station 41008 wind velocity time series at 80 meters (V_{80}) for late March up to early June 1988. **Bottom panel:** Station 41008 power production computation for the *GE3.6s* wind turbine. The dashed line represents its historical (~11 years) average value (~1.08 MW). Note the large variations on the scale of days.

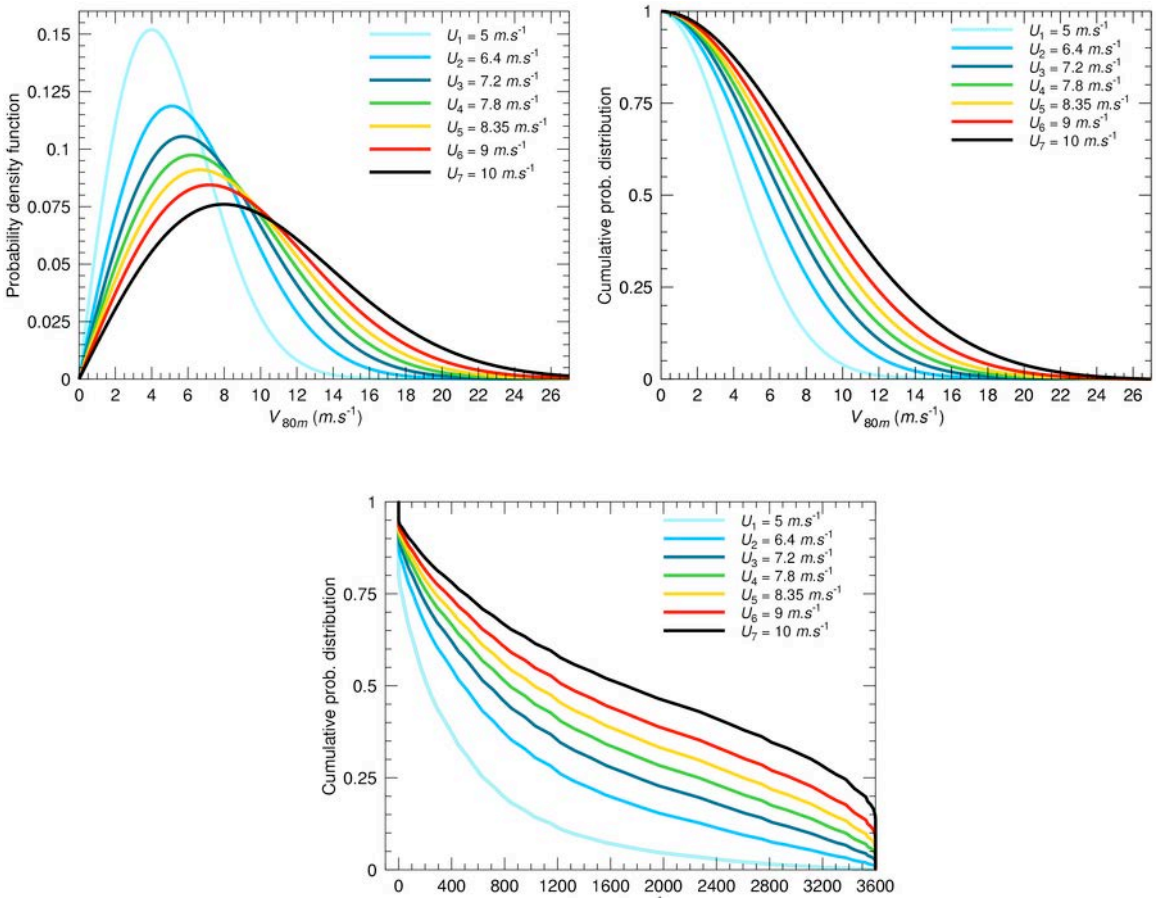

Figure 14) Top left: Rayleigh wind speed probability density function for each wind class. **Top right:** Cumulative probability distributions derived by the integration of the Rayleigh pdf's curves. **Bottom:** Power production cumulative probability distribution for each wind class, based on the *GE3.6s* power curve. Note that the average speed values are indicated in the legend.

In order to better estimate the "amount" of time we are expected to generate a certain "amount" of power, we turn to the probability analysis. The main idea how to obtain a cumulative probability curve for a turbine power production was explored in the methods section. Now with the purpose of analyzing the potential efficiency of our wind sites for the Florida coast, we summarize the analyses in terms of wind classes.

Following the wind class distribution proposed by Archer and Jacobson (2003) presented in Figure 6, we selected average values for each of the 7 wind classes to build up their probability distributions based on the Rayleigh expression given by Equation 5. The resulting functions are shown in Figure 14 (top left panel).

As expected, larger values of mean wind speed give higher probability at higher wind speeds. The specific average value represented by each line is depicted by the legend. They range from 5 to 10 $m.s^{-1}$. The following graph (right top panel, Figure 14) present the cumulative probability distributions as a function of wind speed for each one of the classes, and the bottom graph is finally our cumulative probability distribution function in terms of "generated power" by the wind turbine.

The last graph gives us a good way for analyzing the power production probability for each station already classified in the colored hexagons of Figure 6. By simple visual inspection we can access an estimate of the minimal production. In Table 2 we display the power production respective to 25, 50 and 75% probability.

Prob./Class	C1	C2	C3	C4	C5	C6	C7
25%	633 KW	1327 kW	1833 kW	2272 kW	2614 kW	2933 kW	3305 kW
50%	205 kW	452 kW	633 kW	852 kW	1031 kW	1221 kW	1704 kW
75%	32 KW	108 KW	169 kW	204 kW	290 kW	349 kW	519 kW

Table 2) Minimal power production for different wind classes and probabilities.

Some caution must be given prior to any analysis. The correct meaning of these probability values must be understood as a "conservative estimation". Namely it represents the percentage of time the turbines will be generating *at least* this amount of power. Information is given about an upper bound.

Therefore, even though Jacksonville's offshore stations present an average power production of 1131 MW and 1331 MW, the analysis of their wind classes with the probability curves indicates that they will produce at least 1833 kW and 2272 kW 25% of time. For more conservative analysis, that will be a power generation of at least 169 and 204 kW 75% of the time.

4) Extreme meteorological events

Hurricanes and tropical storms are a big issue in Florida, largely affecting land and sea[**]. Damage caused by these extreme meteorological events is felt on man made structures on the coast and the same effect is expected for offshore wind turbines. The effects on the structure of offshore wind turbines include strong winds but also an increase in waves loads. New turbine design try to overcome these constraints. There are a variety of reasons to keep the weight of the components low. On the other hand, the resulting turbine must be strong enough to survive any likely extreme event and operate reliably with a minimum of maintenance for a long time (McGowan & Connors, 2000).

Manwell et al. (2005) have discussed the effects of wind and waves loads on wind turbine structures and pointed out the main factors involved. Wind acts through lift and drag force on various parts of the turbine and the tower. Wave loads are less well known in the wind industry and consideration is given to the drag component and the inertial component affecting the foundation. The combined effect however, is not well known and there is the need for further research.

So far no offshore wind farms have been built in potential hurricane affected regions although wind farms exist in the mid-western U.S., withstanding tornados. In the Caribbean, land based wind farms are already operating, for example in Curacao, Costa Rica, Jamaica and Cuba.

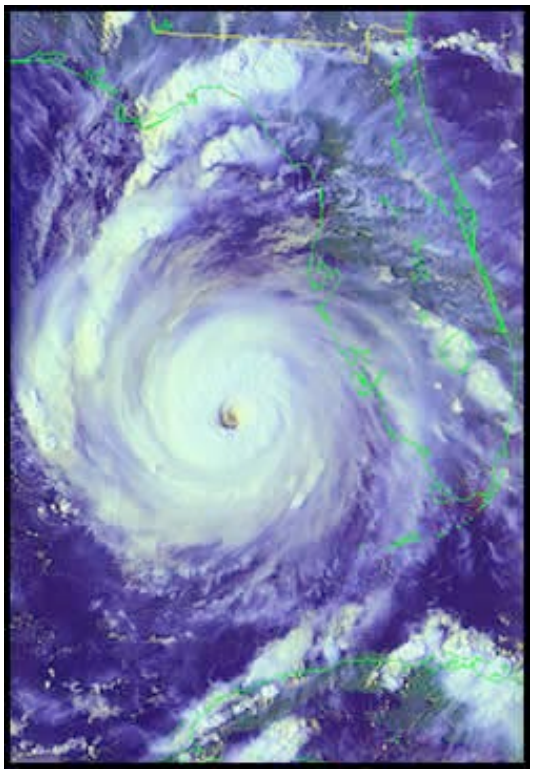

Figure 15) Hurricane west of Florida. Note the size of the hurricane compared to the state (denoted by the green line)

In Cuba the U.S. Naval Station in Guantanamo Bay installed four turbines at 80 meters height, as published by the American Forces Information Service News Article in March 2005. They are anchored in a block of concrete through which 22 soil anchors are sunk 30 to 40 feet deep into the mountain. These wind turbines are rated to withstand winds up to 140 miles per hour, which is equivalent to a Category 4 hurricane[††].

In Jamaica, the Petroleum Corporation of Jamaica constructed a wind farm consisting of 23 wind turbines, which can produce 900-kilowatt with a hub height of 49 m using NEG Micon wind turbines[‡‡]. NEG Micon, a Dutch wind turbine manufacturer, produces wind turbines, which are strong performers at high wind speed sites and are available in three different configurations (standard, arctic and tropical)[§§].

The maps in Figure 16 contain data obtained from the NOAA website on extreme events that reached Florida from 1973 to 2003. At first look at the large number of hurricanes and storm tracks in the upper figure any attempt seems to be impossible to implement a wind farm in this region. However, considering the use of the same turbines used in Guantanamo Bay and assuming the same resistance up to a Category 4 hurricane, the tracks are cleaned and just really strong events would damage the wind turbines as shown in the lower figure.

The passage of a hurricane of such magnitude is known to have several effects that are felt far from these thin tracks. Figure 15, from a satellite image gives an idea about the spatial extent of an event like this. But

[**] http://www.nhc.noaa.gov/
[††] http://www.defenselink.mil/news/Mar2005/20050329_342.html
[‡‡] http://www.pcj.com/wigton.htm; www.mct.gov.jm/Wigton%20Wind%20Farm%20-%20Minister.pdf
[§§] http://www.poweronline.com/content/productshowcase/product.asp?docid=da10ee3c-f729-11d4-a770-00d0b7694f32&VNETCOOKIE=NO

even if the tracks do not provide a very helpful framework to understand qualitatively the influence of extreme events, at least it makes it possible to quantify the incidence of hurricanes in the Florida area in a 30-year period.

To look at offshore structures it is possible to compare a wind turbine with the NOAA station FWYF1 that has a height of 43.9 m (see Figure 5), and continuously collected data from 1991 to 2004, therefore being stable enough to withstand hurricane force winds.

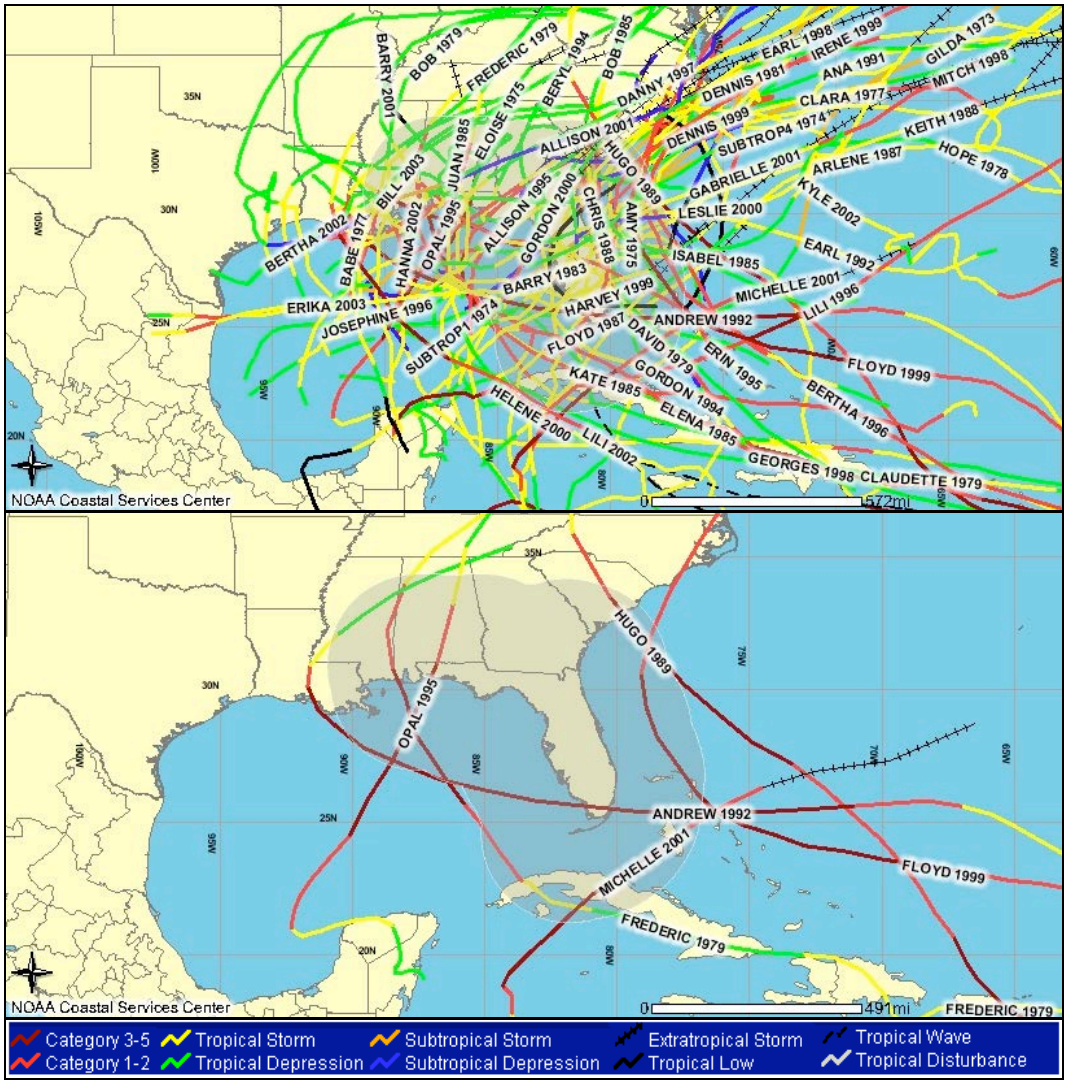

Figure 16) Extreme event tracks obtained from NOAA for the Florida area from 1973 to 2003. **Upper map:** all storms. **Lower map:** Category 4 and stronger hurricanes only.

According to estimates made by Huang et al. (2001) using simulation techniques to statistically characterize the long-term hurricane risk in a 50-year mean recurrence interval (MRI) the gradient wind speed ranges from 60 to 68 $m.s^{-1}$ in Florida. The probability of exceeding this N-year MRI wind speed is given by $1-(1-(1/N))^m$, where m is the number of years of interest. This calculation was made by Huang et al. to evaluate buildings damage and losses but here we propose its use to estimate the effects on wind turbines. Maybe the same approach could be made for wind turbines with appropriate considerations. Wind turbines designed today are expected to have an average 20 year lifetime and the probability of them facing an extreme event such as a hurricane could be estimated. However these calculations need some more information that are not going to be addressed here.

4) Ocean currents as a source of energy

Besides looking at wind energy over land and offshore wind we broaden our view to the energy stored in the ocean. Especially Florida, having good access to strong currents due to the Gulf Stream, can consider their potential for renewable energy sources from the ocean.
In this section we will first explain the equipment and available technology, then explore the currents off the coast of Florida, focusing on the Gulf Stream, and in the end make some calculations regarding the possible energy source from the currents.

4.1) Equipment and available technology

It should be only be a matter of time before structures with new technologies are built that use the ocean's energy. Here we present two possible designs. It might be possible that the marine current industry will develop in the same way in the future the wind power industry did.

The company Ocean Renewable Power Company (ORPC), founded in 2004, recently developed an ocean current generation project. Their modular platform-type facilities will be located below the ocean's surface at about 20 to 50 m depth (see right panel in Figure 17). The modules will be attached to the ocean floor using deep sea mooring systems and will have new configurations of already existing technologies.
For each module the generating capacity will be 4 to 10 megawatt. A typical project will consist of several power modules deployed in an array. These will be interconnected to an on-shore utility substation through an underwater transmission line.
The first commercial project, planned to be completed by mid-2008, will produce 48 MW; following projects are planned to be two to three times larger than this, producing 100 to 200 MW.

The advantage of ocean currents in comparison to wind is their stability since they are flowing continuously. Unlike many other renewable energy resources, ocean currents are able to provide a reliable and base-loaded energy supply, in comparison to the intermittent power supply that wind power provides.

As another example of how to use the energy of the ocean, tidal stream turbines as constructed by Marine Current Turbines Ltd. (MCT) are worth mentioning (see left panel in Figure 17)[***].

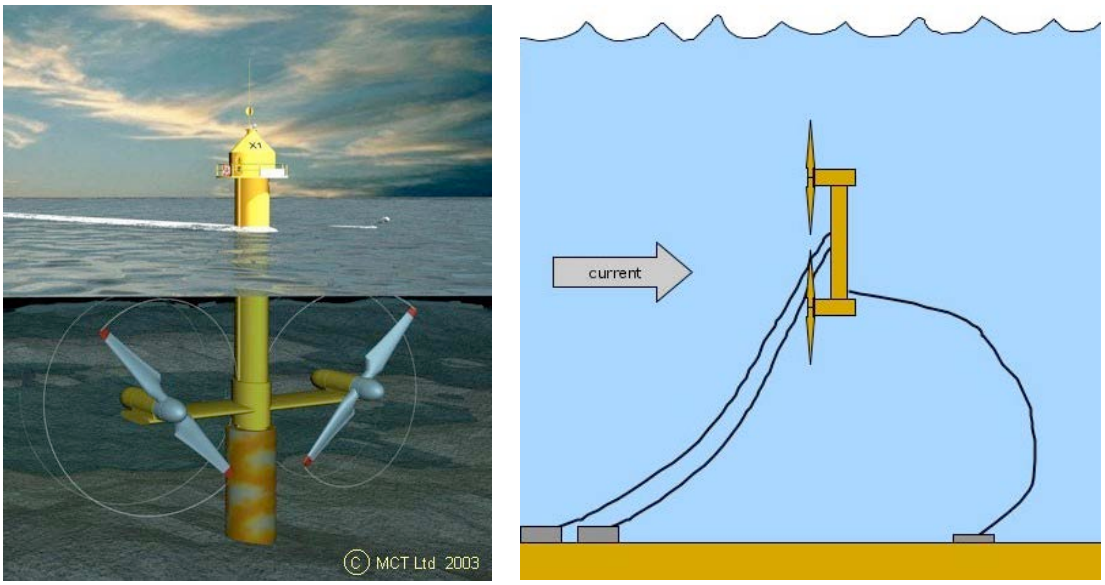

Figure 17) Left Panel: MCT pile mounted twin rotor tidal turbine[***]. **Right Panel:** Sketch of an orpc ocean generation module

[***] http://www.marineturbines.com

These turbines, composed of twin axial flow rotors of 15 to 20 m in diameter, take advantage of high tidal currents. The installation of the first small tidal turbines (four to five units) took place in 2004 - 2005, which gives an aggregated power for the system of about four to five MW.

In this study we will just focus on the modules produced by ORCP because they are designed for ocean currents, but it is important to point out that there are more possibilities and many companies are working on renewable energy from the ocean.

4.2) Currents off the coast of Florida

ORCP picked six different project sites for development, all off the southeast coast of Florida, fitting well with our research of renewable energy for Florida. So this paper will take a closer look at currents and options concerning those.

In order to examine the ocean currents in the Gulf Stream in the Florida area, results from Hamilton et al.'s paper from 2005 will be presented, in which transports for sections of the Florida Current from Key West to Jupiter in the southeast of Florida were calculated. Moored current-meter arrays as well as voltages from cross-channel telephone cables were used for the estimates.
The map in Figure 18 shows the area the paper is focusing on and we will especially pay attention to mooring arrays C and D (red circles in map).

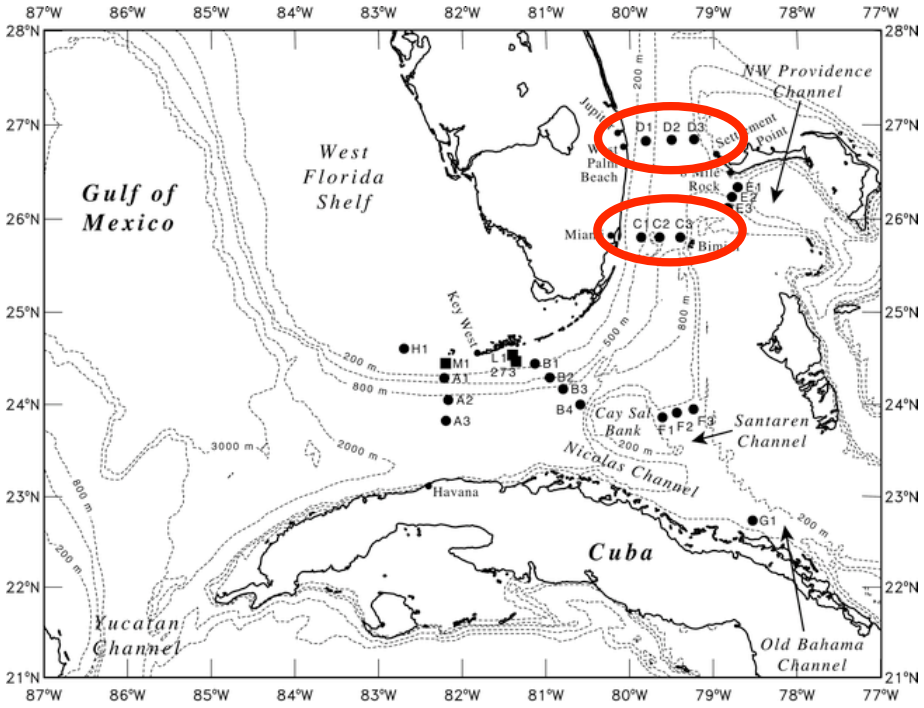

Figure 18) Map of the mooring positions for the Straits of Florida study (dots) and SEFCAR (squares) with areas specified in the text circled (from Hamilton et al. 2005).

Figure 19 shows the along channel current velocity at section D over time for one year from November 1990 to November 1991 for stations D3, D2 and D1 from top to bottom in $cm.s^{-1}$. Focusing on the red line, which is the measurement closest to the surface, currents of around 50 – 100 $cm.s^{-1}$ can be observed. Values for D1 rarely drop below the 75 $cm.s^{-1}$ line. These currents are rather stable, reaching highest values closer to the shore (D1). This gives even more confidence in building a "current generation module park" since the area needs to be in reasonable distance to the coastline to reduce transmission losses.

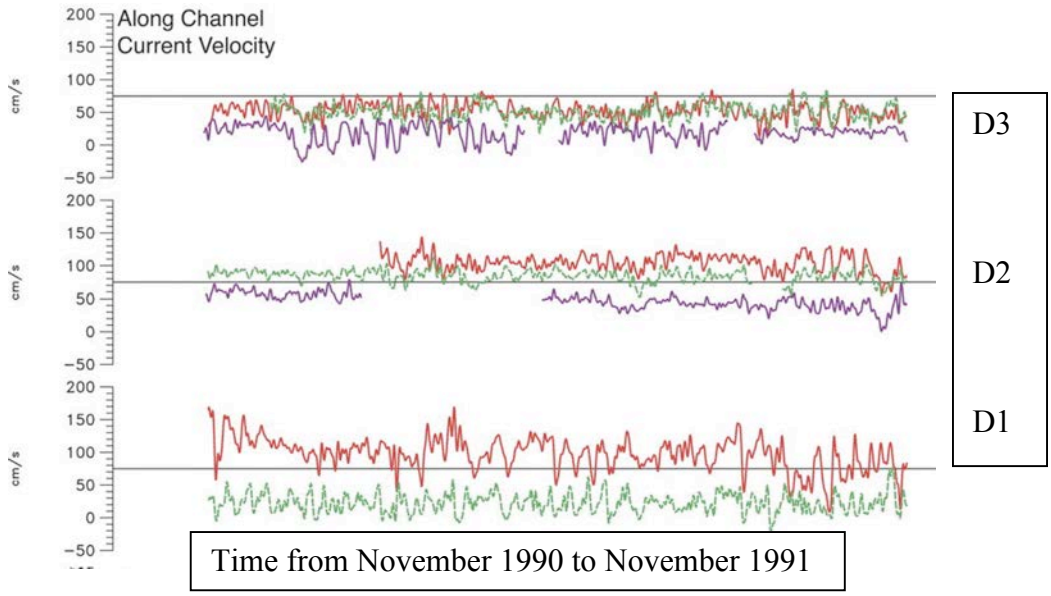

Figure 19): Along-channel 40-h low passed filtered velocities on section D. Nominal measurements depth is 145 meters (red), 300 (green dashed), and 600 m (purple) (from Hamilton et al. 2005).

In Figure 20 the monthly mean transports for sections A (Key West – Havana cable), C (Miami – Bimini) and D (Jupiter – Settlement Point current meters) of the Florida currents are shown. Looking at sections C and D again, denoted by the light and medium gray bars, the transport throughout the year never drops below 26 Sverdrup (1 Sv ≡ 10^6 m^3s^{-1}). Seasonal changes barely exist, making currents an even better source for energy, since changes on a daily, weekly and monthly basis do not occur on such an abrupt basis as wind does, never dropping to zero.

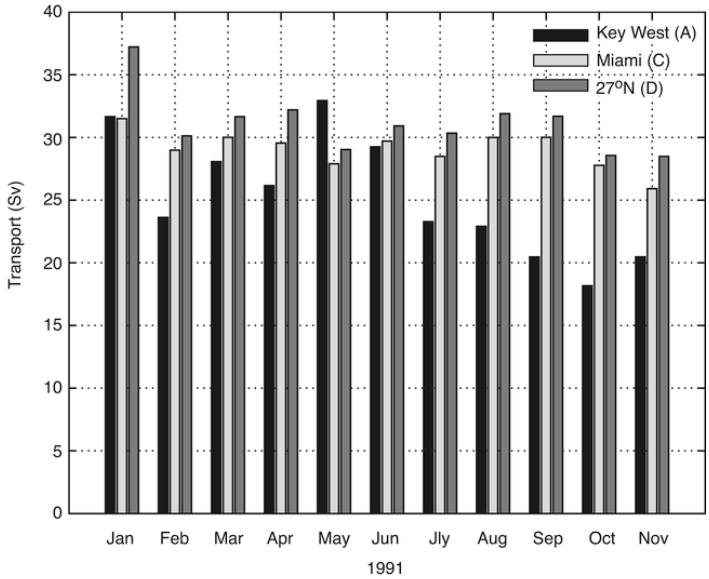

Figure 20) Monthly mean transports (centered on the first of the month) for sections A (Key West – Havana cable), C (Miami – Bimini) and D (Jupiter – Settlement Point current meters) of the Florida currents (from Hamilton et al. 2005).

4.3) Calculations regarding energy sources from currents

Making comparisons between offshore wind energy and current energy, it is important to note that the densities of both fluids, air and water, are very different. Density of air is 1.225 kg.m^3 while the density of saltwater at 20°C and 30 PSU is 1020 kg.m^3. The assumption can therefore be made that water is about 832 times denser than air (1020 kg.m^3 / 1.225 kg.m^3 = 832). The equation for the kinetic energy with v = velocity and ρ = density is:

$$KE = \frac{1}{2} * \rho * v^2 \qquad \text{(Eq.6)}$$

It is possible to make an assessment of how fast water must be flowing to have the same amount of kinetic energy as air. That way an underwater ocean current module can be compared to an offshore wind farm.

Comparing the kinetic energy of water with that of wind gives the following equations and results:

$$KE(water) = KE(air)$$

$$\frac{1}{2} * (832) * \rho * v_{water}^2 = \frac{1}{2} * \rho * v_{air}^2 \qquad \text{(Eq.7)}$$

$$v_{water}^2 = v_{air}^2 / 832$$

$$v_{water} = v_{air} / 29$$

Therefore the velocity of water has to be 1/29th that of air to have the equivalent amount of kinetic energy. Having current speeds of an average of 100 cm.s^{-1} = 1 m.s^{-1} in the Gulf Stream off the coast of Florida (see Figure 19), this is equal to mean wind speeds of almost 30 m.s^{-1} during the whole year. Not only are the continuous aspects about wind unrealistic, but high wind speeds like this over longer times are also unrealistic. Therefore it is even more obvious that there is much more kinetic energy in the ocean, due to the higher density of water.

It should be kept in mind that real fluid dynamics is more complicated than this. For a crude estimate this at least gives an impression of the potential that currents in the oceans have. Note that kinetic energy is more useful when it is expressed as kinetic energy per unit volume.

In the following we present calculations for power as were already described in Equation 2.

$$P = A * \frac{1}{2} * \rho * (v)^3 \qquad \text{(Eq.8)}$$

$$A = \pi * R^2$$

For the power production from currents, assumptions are made for different swept areas since it is not clear how the blades for underwater use will be designed. We picked values ranging from 2.5 m as radius to 20 m radius, giving us swept areas from 20 to 1256 m^2. The reason for these values is suggested by MPI for rotor diameters of 15 to 20 m. This can also take into account modules with separate units as can be seen in the right panel of Figure 17. Assuming four small units, we can assume a bigger radius value to represent the whole module rather than just one unit. For wind blades the swept area of 8495 m^2 was taken from the *GE3.6s* turbine. The density values given above were used. Speed of the water varied ranging from 0.5 m.s^{-1}, which would be suitable even at less energetic sites than the Gulf Stream, to a reasonable value of 1 m.s^{-1} for the Gulf Stream up to 1.5 m.s^{-1} as optimistic peaks in the current velocity. Wind velocities occur in the Florida region in wind classes three to four, giving average wind speeds of about 7.5 m.s^{-1}. Calculations were made for 5, as an example for less optimal sites, 7.5 and 10 m.s^{-1} as a very good site.

The results of the calculations are given in the following Tables 3 to 5. In Table 3 the three different current velocities are applied to the varying swept areas, given in terms of the radius. Extreme values of 1,251 to 3,379,666 were calculated. But it would be most realistic to expect current value around 1.0 m.s^{-1} for the Gulf Stream. The smallest blade radius is not really representative when compared with one wind turbine since more units will be combined in one module.

v_{water}/radius	2.5 m	5 m	10 m	15 m	25 m
0.5 m.s^{-1}	1,251	5,006	20,027	45,062	125,178
1.0 m.s^{-1}	10,013	40,055	160,221	360,497	1,001,382
1.5 m.s^{-1}	33,796	135,186	540,746	1,216,679	3,379,666

Table 3) Power for different current velocities and different radius in water (Watts).

For a better comparison to wind turbines the power of wind was computed, (shown in Table 4), for the variables explained above.
Then the ratio between the power obtained from wind turbines to the power obtained from ocean currents is given (Table 5). For 1.0 m.s^{-1} current velocity the ratio drops from 219 for the smallest blade radius to 2 for the biggest radius. Therefore comparing one module consisting of several small units to one wind turbine gives a similar energy resource.

v_{wind}/radius	52 m
5 m.s^{-1}	650,398
7.5 m.s^{-1}	2,195,094
10 m.s^{-1}	5,203,187

Table 4) Power for different wind speed velocities for air (Watts).

v_{water}/radius	2.5 m	5 m	10 m	15 m	25 m
0.5 m.s^{-1}	1,754	438	109	486	17
1.0 m.s^{-1}	219	54	13	6	2
1.5 m.s^{-1}	64	16	4	2	0.6

Table 5): Ratio between power in air for 7.5 m.s^{-1} and water.

The advantage of currents over wind is the continuity achieved, even though the ratio is more in favor of winds. More aspects would need to be considered in comparisons; as for example maintenance costs, etc. But wind and currents should not be seen as competitive energy sources anyway. Rather they should be seen as supplement sources of energy, especially since continuous and non-continuous sources make good combinations.

5) Marine Protected Areas (MPA)

By the U.S. official definition, a marine protected area is "any area of the marine environment that has been reserved by federal, state, territorial, tribal or local laws or regulations to provide lasting protection to part or all of the natural or cultural resources therein". This is only a general definition, since there could be different classifications of MPAs, as well as different levels of protection[†††].

The Florida's MPAs are shown in Figure 21. The state of Florida has 41 aquatic preserves (37 located on the coast), three National estuarine research reserves (the Apalachicola National Estuarine Research Reserve, the Guana-Tolomato-Matanzas National Estuarine Research Reserve and the Rookery Bay National Estuarine Research Reserve) and one National marine sanctuary (the Florida Keys National Marine Sanctuary).

Figure 21) Marine protected areas of Florida
(http://www.dep.state.fl.us/coastal/programs/aquatic.htm)

The Florida Aquatic Preserves Program was established in 1975, by the State's Aquatic Preserve Act. This program is under the Department of Environmental Protection, and it manages the aquatic preserves as well as the National estuarine research reserves. In general, the program restricts alterations and developments, as well as future leases or sales of submerged lands, within the aquatic preserves system, unless a proposal is considered to be clearly in the public interest[‡‡‡].

National Marine Sanctuaries are areas with distinctive natural and historical resources, which are established for the public's long-term purposes. These areas are administered by NOAA, under the Office of Ocean and

[†††] http://mpa.gov
[‡‡‡] http://www.dep.state.fl.us/coastal/programs/aquatic.htm

Coastal Resource Management. The Florida Keys National Marine Sanctuary was created in 1990, when the President signed the Florida Keys Marine Sanctuary and Protection Act. The regulations of this marine sanctuary prohibit all activities that involve alteration of, or construction on, the seabed; removal of, injury to, or possession of coral or live rock; movement of, removal of, injury to, or possession of sanctuary historical resources; among others. These prohibited activities would certainly be conflicting with the activities necessary for the construction of a wind farm.

Another area of interest related with MPA in Florida is the proposed area for the management of right whales (*Eubalaena glacialis glacialis*), on the northern coast of Florida (Figure 22). The population of right whales which lives along the east coast of the North Atlantic Ocean is considered to be critically endangered. The northern coast of Florida is used by this population of right whales as a calving area, from December through March. Even though this is only a proposed area, the impact of a wind farm, especially during the construction of the site, has to be considered[§§§].

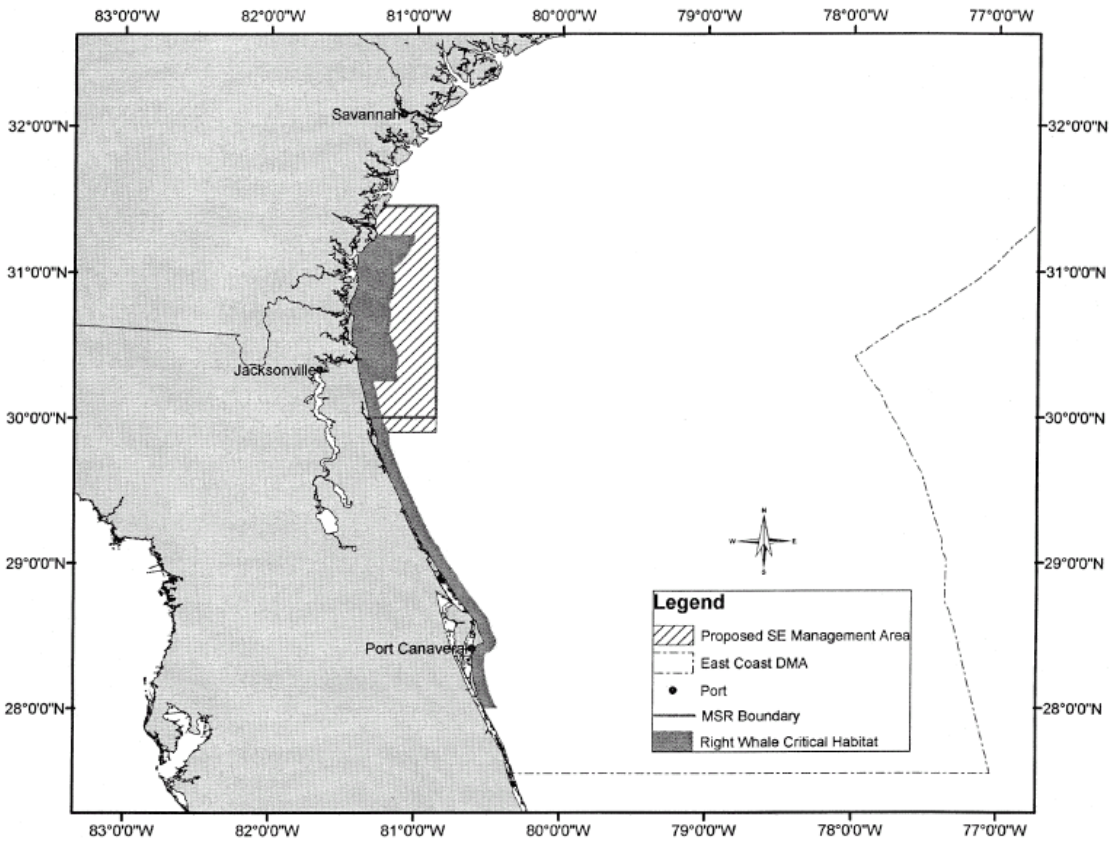

Figure 22) Proposed area for the management of right whales; (from: Federal Register / Vol. 69, No. 105 / Tuesday, June 1, 2004 / Proposed Rules)

[§§§] http://www.nmfs.noaa.gov/pr/species/mammals/cetaceans/right_whales.doc

6) Summary and Conclusions

The present report made a preliminary evaluation on offshore wind and ocean currents for the state of Florida, United States, from the point of view of renewable energy resources. The technologies associated with the wind generation of power available at this point already permit the "harvesting" of wind energy in offshore areas, where the resource is typically more abundant than in continental areas. We have made the use of all historical wind data available from the National Data Buoy Center for the Florida coast in our analysis. The analysis suggests that the offshore wind resource for Florida is situated from classes one up to four, with power density values between 100 and 500 $W.m^{-2}$.

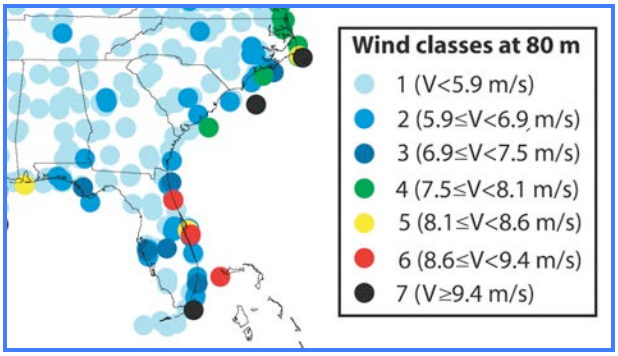

Figure 23) Continental wind power classification given Archer & Jacobson (2003).

Most of the class one and class two stations are located in the west, in the coastal areas between 27° and 30° N latitude. These stations have strong continental boundary influence, since they are situated over land. At the same time, the large distance of the buoys from the coast precludes a good estimation of the wind over this inner-shelf area. The class three occurred all along the east inner-shelf between 26° and 32°N latitude and on the extreme west coast, around Panama City. These places demonstrated turbine activity higher than 80%. In terms of production, the joint analysis of the *GE3.6s offshore wind turbine* power curve with our wind data allowed us to identify the class three sites as the best places for wind power generation ranging from an average production of 1 MW for Miami to about 1.15 MW for Jacksonville and Pensacola inner-shelves. For Key West, the only class three station was located near the end of the archipelago. The average turbine power production along the archipelago ranged between 0.7 and 1.0 MW. The class 4 sites were located in deep waters and represent a future challenge for the installation of wind turbines.

Average values of turbine production for the west coast inner-shelf evaluated for a wind farm of 130 turbines (comparable number to Cape Cod project) resulted in an average power production of 169 MW. Considering high productivity periods (25% of time, see Table 2) a farm production could achieve approximately 238 MW for class three and 295 MW for class four. In terms of the *minimum production,* expected at 75% of time, we would obtain low values as 21.97 MW for class three and 26.52 MW for class four. These are very conservative estimations though, as explained before. In comparison to our values for Florida, the Cape Cod project evaluated a *total* *maximum* output of 420 MW (nearly 3.23 MW per turbine) which corresponds nearly to 40% higher productivity than our class four stations (with 25% probability taken as maximum production).

It might be interesting to observe that the estimated resource offshore of the Florida coast was consistently higher than estimated for the continental areas by Archer & Jacobson (2003) (compare Figure 23 with Figure 9). Overall they found class one winds over the continent and some higher classes, up to class five and six in some coastal stations. This suggests the offshore resources estimated in this work are at least 2 classes higher than wind over the continent. Another interesting point is that Archer & Jacobson's (2003) method on the extrapolation of wind speeds to 80 m height was based on the least square fit based on twice-a-day wind profile from meteorological soundings. This method results in 80 m winds speeds that are, on average, 1.3 to 1.7 $m.s^{-1}$ faster than those obtained from the log law we have applied. This means that our results can be underestimating the actual wind power for Florida, suggesting that further investigations should be attributed to increase the precision on the estimation of offshore wind vertical profiles.

As reasonable candidates for the placement of offshore wind farms, we list Pensacola, Miami and Jacksonville coasts that are near densely populated areas. Here we exclude Key West from this list not only because of the relatively lower wind resource, but also due to the large area occupied by the *Florida Keys National Marine Sanctuary* (Figure 21). From a practical point of view, perhaps the best candidate would be the area close to Jacksonville. Jacksonville is the 14th largest city in the United States, with a population of more than

800,000 people, and it has the largest urban park system in the country. As seen, this region has a reasonable wind resource, with an average of 7 to 8 $m.s^{-1}$ winds at the inner-shelf and 80 up to 85% of turbine activity. But the main advantage of Jacksonville is that it has some kind of RPS. In 1999, the JEA (the Jacksonville metropolitan area utilities company) signed a memorandum of understanding with the Sierra Club and the American Lung Association regarding renewable energy generation. The goal of this memorandum is to have 7.5% of the energy coming from renewable sources by 2015. Although the Guana-Tolomato-Matanzas National Estuarine Research Reserve is close to the area, it could be avoided in a project of a wind farm. This region has the wind resources and the market for offshore wind power, and with further studies environmental issues could be evaluated.

Hurricanes and other extreme events are an issue of major concern in Florida, for any construction near the shore and especially offshore. However, turbine design engineering is being developed to withstand more rigorous conditions. The actual feasibility for an implementation of a wind farm is not well defined since more studies are needed on the probability of occurrences of storms and hurricanes and on the behavior of wind turbines facing these extreme events. Though, the overcome of these constraints seem to be a matter of time.

As an alternative to wind energy, this study also focused on currents, especially off the east coast of Florida. High current velocities occur within part of the Gulf Stream. The analysis of new technologies and comparisons to wind turbines lead to the conclusion that ocean currents are not necessarily an alternative but rather a supplement to wind power. Being more reliable, ocean currents can provide a constant base-load in comparison to intermittent power supply from wind. One downside of the ocean current modules will be the discussion if the modules endanger marine life as wind turbines interfere with birds and bats. So far no empirical information exists because these modules are the first of their kind. The company ORPC claims that the slow revolution speed of the blades will not endanger marine life but this will need to be proven. With all the other advantages though, ocean current power generation should be considered as an additional energy source.

Although the current technologies for ocean current energy are still under development, for a near future a well-suited candidate for the "ocean park" for the generation of power is the Miami coast. The region has a steep continental shelf with the resource of currents not very far from the coast (the 500-m isobath is less than 30 km from the coast). This short distance would help to lower the cost of maintenance and power transmition losses. For this area, the combination of wind and ocean currents would provide sustainable and clean resources for present and future generations, perhaps using the same underwater transmition lines.

Finally, a study realized by the Florida PIRG Education Fund in 2005 pointed out the economic and public benefits of the use of renewable sources of energy for the state. Two policies were considered: a RPS of 20% by 2020 and the shifting of the Florida's costs to subsidize the fossil fuels and nuclear power ($1.6 billion) towards renewable energy and energy efficiency. By implementing these two policies, a net annual average of 4,237 jobs would be created between 2005 and 2020; the state's gross product would increase by an annual average of $40 million between 2005 and 2020; consumers would save $760 million on electricity bills in 2020; there would be a reduction of global warming carbon dioxide emissions from power plants by 15% of 2002 levels. These results also demonstrate the economical importance and benefits of the implementation of renewable sources of energy in Florida.

7) References

Archer & Jacobson (2003). Spatial and temporal distributions of U.S. winds and wind power at 80 m derived from measurements. *Journal of Geophysical Research,* V.108 D9, doi:10.1029/2002JD002076.

Bailey B. & Brennan S. (2004). Making the case for offshore wind energy development in the U.S. – A comparison of land versus offshore potential. *Global Windpower Conference,* Chicago (Online at: http://www.ocean.udel.edu/windpower/ResourceMap/index.html).

Caldeira K. & Wickett M. E. (2003). Anthropogenic carbon and ocean pH. *Nature*, V. 425, p 616.

Church J. K. et al. (2001) in Climate Change 2001: The Scientific Basis Contribution of Working Group I to the Third Assessment Report of the Intergovernmental Panel on Climate Change (eds Houghton J. T. et al.) 639-693 (Cambridge Univ. Press)

Gregory J. M., Huybrechts P. & Raper, Sarah C. B. (2004). Threatened loss of the Greenland ice-sheet. *Nature,* V.428, p 365.

Hamilton P. et al. (2005) Transports through the Straits of Florida. *Journal of Physical Oceanograph*y, V.25, p 308 – 322

Huang Z., Rosowsky D. V. and Sparks P. R. (2001). Long-term hurricane risk assessment and expected damage to residential structures. *Reliability Engineering and System Safety*, V.74, p.239-249.

Manwell J. F., McGowan J. G. and Rogers A. L. (2002). Wind energy explained: Theory, Design and Application. *West Sussex: Wiley.*

Manwell J. F., Elkinton C. N., Rogers A. L. and McGowan J. G. (2005). Review of design conditions applicable to offshore wind energy in the United States, *Renewable and Sustainable Energy Reviews*, article in press.

McGowan J. G. & Connors S. R. (2000). Windpower: A Turn of the Century Review, *Annual Review Energy Environment*, V. 25, p 147-197.

Nayak, N. (1995). Redirecting Florida's Energy: The Economic and Consumer Benefits of Clean Energy Policies. Florida PIRG Education Fund.

Huang Z., Rosowsky D. V. and Sparks P. R. (2001). Long-term hurricane risk assessment and expected damage to residential structures. *Reliability Engineering and System Safety*, V.74, p.239-249.

Hurley, P. (2005). State Renewable Portfolio Standards. Nelson A. Rockefeller Center, Dartmouth College

Federal Register (2004) Proposed Rules, Vol. 69, No. 105

NOOA (1996), Florida Keys National Marine Sanctuary Final management plan/Environmental impact statements, Vol. 1.

oceanrenewable power company (March 2005) Generating Electricity from Ocean Currents